J. Biochem. 2009;145(6)799–810
doi:10.1093/jb/mvp039

Effective Induction of Cell Death on Adult T-Cell Leukaemia Cells by HLA-DRβ-Specific Small Antibody Fragment Isolated from Human Antibody Phage Library

Satoshi Muraoka[1], Yuji Ito[1,*], Masaki Kamimura[1], Masanori Baba[2], Naomichi Arima[2], Yasuo Suda[3], Shuhei Hashiguchi[1], Masaharu Torikai[4], Toshihiro Nakashima[4] and Kazuhisa Sugimura[1]

[1]Department of Bioengineering, Faculty of Engineering, Kagoshima University, Korimoto 1-21-40, Kagoshima, Kagoshima 890-0065; [2]Center for Chronic Viral Diseases, Graduate School of Medical and Dental Sciences, Kagoshima University, Sakuragaoka 8-35-1, Kagoshima, Kagoshima 890-8544; [3]Nanostructured and Advanced Materials Course, Graduate School of Science and Engineering, Kagoshima University, Korimoto 1-21-40, Kagoshima, Kagoshima 890-0065; and [4]The Chemo-Sero-Therapeutic Research Institute, Kyokushi, Kikuchi, Kumamoto 869-1298, Japan

Received December 19, 2008; accepted February 23, 2009; published online March 6, 2009

By a biopanning method using cell sorter, we quickly isolated an antibody phage clone (S1T-A3) specific to human T-lymphotropic virus type 1-carrying T-cell line S1T from a human single chain Fv (scFv) antibody phage library. This scFv antibody bound to HTLV-1-carrying T-cell lines including MT-2, MT-4 and M8166 other than S1T, but not to non-HTLV-1-carrying T-cell lymphomas such as Jurkat and MOLT4 cells. Interestingly, this antibody induced the cell death on S1T cells very quickly (<30 min). We tried to identify the target molecules by western blotting and mass spectrometric analysis, revealing that the target antigen was HLA class II DR. The cell death was induced only in dimmer form of scFv (diabody) and at 15-fold lower concentration than that of a fusion protein of scFv and human IgG Fc [$(scFv)_2$-Fc] or anti HLA-DR mouse whole antibody L243. Thus, S1T-A3 diabody is a small antibody fragment with agonistic activity to induce cell death through HLA-DR. This is the first report elucidating that diabody specific to HLA-DR is effective to induce the cell death in T-cell malignancy especially adult T-cell leukaemic cell line.

Key words: adult T-cell leukaemia, human antibody, scFv, phage library, diabody.

Abbreviations: APC, antigen presenting cells; ATL, adult T-cell leukaemia; FACS, fluorescence-activated cell sorter; FBS, fetal bovine serum; FITC, fluorescent isothiocyanate; HLA, human leucocyte antigen; HTLV-1, human T-cell leukaemia virus type 1; mAb, monoclonal antibody; MHC, major histocompatibility complex; PE, phycoerythrin; PI, propidium iodide; RMF, relative mean fluorescence; scFv, single chain Fv; SPR, surface plasmon resonance.

ATL (adult T-cell leukaemia) is a disease, which is caused by infection of the retrovirus HTLV-1 (human T-cell leukaemia virus type 1) to $CD4^+$ T cells. As many as 10–20 million people worldwide are estimated to carry the virus (*1*, *2*). Other diseases caused by HTLV-1 infection include HAU (HTLV-1 associated uveitis) and HAM/TSP (HTLV-1-associated myelopathy/tropical spastic paraparesis), which is a neuro-degenerative disease. Although the frequency of ATL development in the life of the carriers is low (2–6%), its prognosis is generally severe after the development of ATL (*2*). Nevertheless, a human antibody for therapeutic use of ATL has not yet been established until now.

The antibody phage library has become a major technology that directly isolates human antibodies for therapeutic use (*3*), along with hybridoma technology using trans-chromosome mouse (*4*). In cell panning to isolate the cell-specific phages by antibody phage display library, several methods were developed to remove non-specific phages, for example, by washing the cells with repeating centrifugation and suspension (*5*), by recovering the cells with magnet beads (*6*) or by sedimentation of the cells though centrifugation in organic solvent (*7*). We employed here another panning method using cell sorter (*8*, *9*) for rapid isolation of the binders and for less damage giving the cells. Furthermore, by use of the control cells as absorber, we could obtain the antibody phages which recognize the unique antigens expressed specifically on the target cells, facilitating the finding of novel tumour markers (*10*, *11*).

We isolated a human scFv antibody specific to S1T cells, a cell line derived from an ATL patient (*12*) by a cell panning method using a cell sorter from a single chain Fv (scFv) human antibody phage library. Interestingly, the obtained scFv antibody induced a cell death on S1T cells within in a very short time (<30 min). In this report, we identified the antigen on S1T cells targeted by this scFv and elucidated the molecular structures which is essential for inducing the cell death. The antibody isolated here can be expected as small therapeutic antibody to kill the malignant T cells.

*To whom correspondence should be addressed. Tel: +81-99-285-8346, Fax: +81-99-285-8346, E-mail: yito@be.kagoshima-u.ac.jp

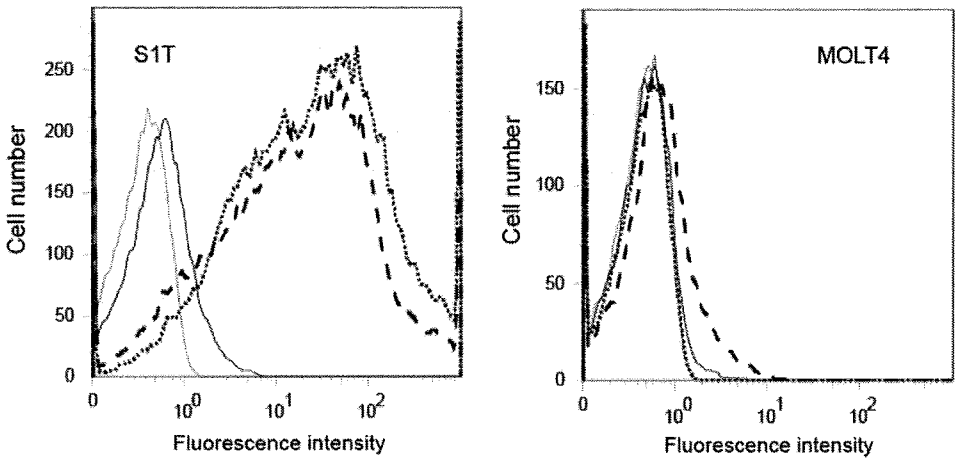

Fig. 1. **The enrichment of the S1T cell-specific phages by cell panning on cell sorter.** The binding activities of the phages amplified after each round of cell panning against S1T cells were analysed using FACS. The lines represent the histograms after the first (thick line), second (broken line) and third round (dotted line) of cell panning. The grey line indicates the control data of the cells stained without phages.

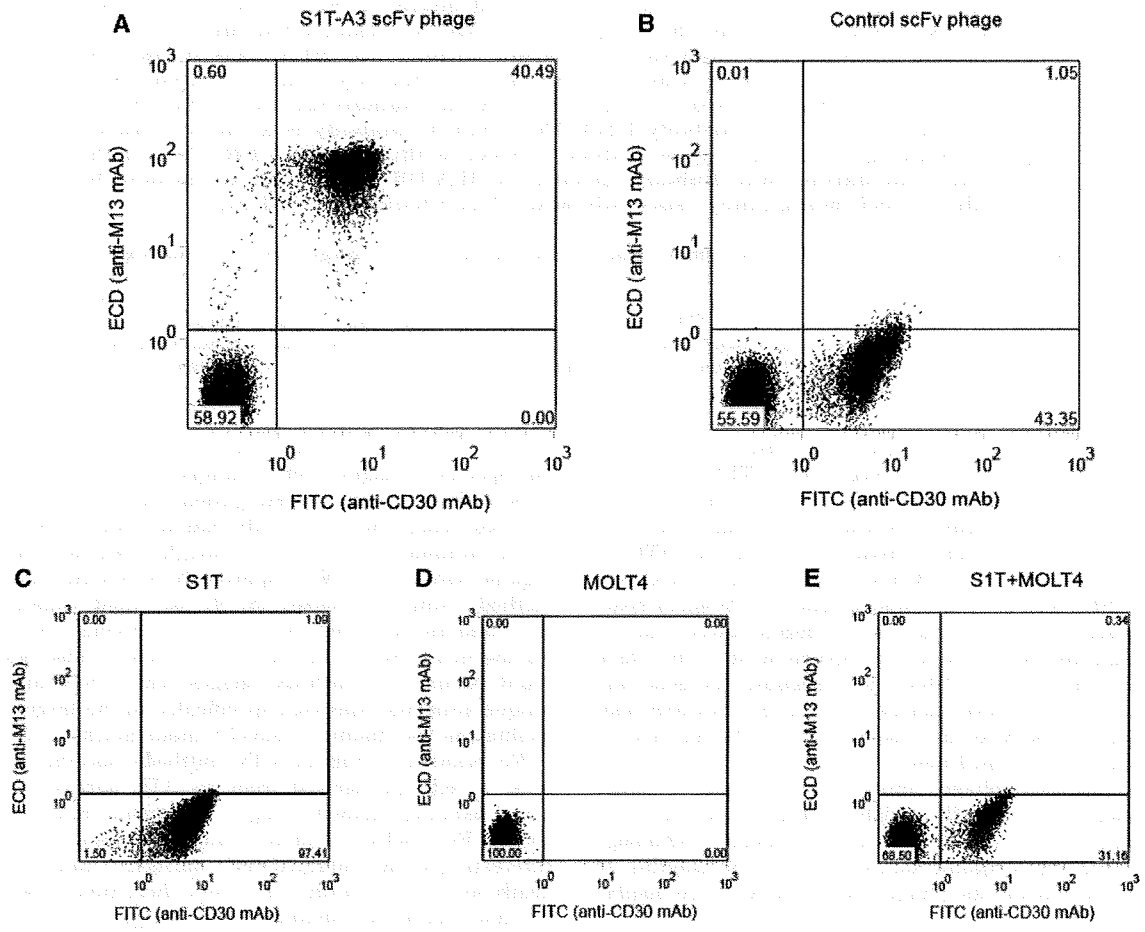

Fig. 2. **The binding specificity of S1T-A3 phage clone to S1T cell.** S1T-A3 (A) or non-specific control (B) phages were incubated with the mixture of MOLT4 and S1T cells, the latter of which were labelled with FITC-conjugated anti CD30 mAb, and analysed on FACS. The other three panels indicate the FACS data for S1T cells labelled with FITC-conjugated anti CD30 mAb (C), non-labelled MOLT4 cells (D) and their mixture (E), respectively.

(a) Amino acid sequence of the VH domain

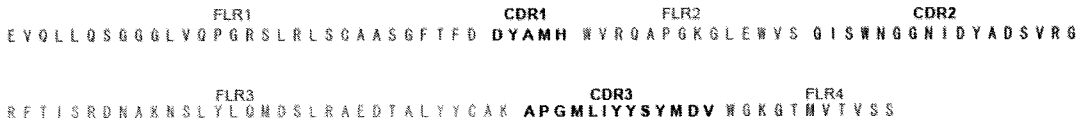

(b) Amino acid sequence of the VL domain

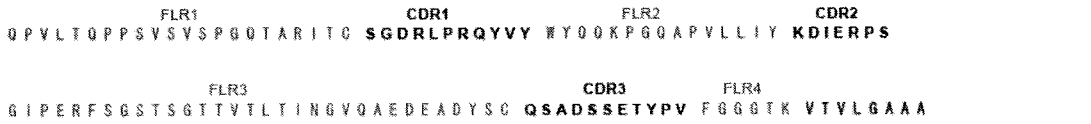

(c) Variable gene usage

	Heavy chain			Light chain	
clone	V	D	J	V	J
S1T-A3	IGHV3-9*01	IGHD3-3*01	IGHJ6*03	IGLV3-25*03	IGLJ3*02

Fig. 3. **The amino acid sequence of the S1T-A3 scFv clone deduced from the DNA sequence.** The complementary determining regions (CDR1–CDR3) and the frame regions (FR1–4) were assigned according to Kabat's numbering. The CDR regions are indicated in bold letters (A and B). The scFv nucleotide sequence was analysed by searching the IMGT/V-QUEST database to identify the gene usage on the immunoglobulin germ line (C) (*35*).

MATERIALS AND METHODS

Cells and Proteins—The HTLV-1-carrying T-cell line S1T was previously established from the peripheral blood mononuclear cells (PBMCs) of an ATL patient (*12*). The other cells used here (HTLV-1-carring T-cell lines: MT-2, MT-4 and M8166; HTLV-1-negative T-cell lymphoma cell lines: MOLT-4 and Jurkat; B-cell lymphoma cell lines: Dauji and Raji) are described in the previous report (*13*). All cell lines were maintained in RPMI 1640 medium supplemented with 10% heat-inactivated fetal bovine serum (FBS), 100 U/ml penicillin G and 100 μg/ml streptomycin. The murine L929 cells (ATCC CCL-1) transfected with the human HLA-DR genes (HLA-DRB*0101 and HLA-DRA*0101) are referred to as L57.23 cells. The purified HLA-DR molecule (DRA*0101/DRB1*0405) was kindly gifted by Prof. S. Matsushita (*10*).

Antibody Phage Library—Human naive scFv phage library with a diversity of 4.5×10^8 was constructed using pCANTAB5E phagemid vector, as described previously (*14*).

Cell Panning on Flow Cytometry—One million S1T cells were labelled with fluorescent isothiocyanate (FITC)-conjugated anti-human CD30 mouse monoclonal antibody (mAb) for 30 min on ice and were washed once with phosphate-buffered saline (PBS). After adding 1×10^6 MOLT4 cells, the cells were suspended in 500 μl PBS containing 1% BSA and were incubated with the scFv-phage library of 1×10^{12} TU (transforming unit) at 4°C for 1 h, with gentle shaking on a rotator. After centrifugation (500*g*, 30 s), the cells were re-suspended in PBS containing 2% FBS (2.5×10^5 cells/ml in 8 ml). After filtration through 40 μm Nylon Mech (Kyoshin Rikoh Inc.), the cells were supplied for cell sorting on an EPICS ALTRA HyperSort (Beckman coulter Inc.) with fluorescence emission (512 nm) by excitation at 488 nm. The S1T cells separated by cell sorting were suspended in PBS and treated with 76 mM citric acid solution (pH 2.5) at room temperature for 5 min to dissociate the bound phages. After neutralization with 1 M Tris–HCl (pH 7.4), the cell suspension was transferred to the culture of *Escherichia coli* TG1 in logarithmic growth phase for infection. The scFv-displayed phages were rescued by co-infection with M13KO7 helper phage and purified by polyethylene glycol (PEG) precipitation from the culture supernatant, as described previously (*14*, *15*). This biopanning process was repeated three times. The phages after the second and third round of biopanning were cloned and used for binding analysis on flow cytometry.

Flow Cytometric Analysis—The mammalian cells with 80–90% confluent growth were collected by centrifugation and washed once in cold PBS and twice in FACS buffer (PBS containing 10% FBS and 0.1% sodium azide). The cells (1×10^6 cells) were incubated with the cloned phages or the purified scFv for 30 min. After washing the cells twice with FACS buffer, the phages bound to cells were stained by biotinylated anti-M13 mAb (GE Healthcare) and phycoerythrin (PE)-conjugated

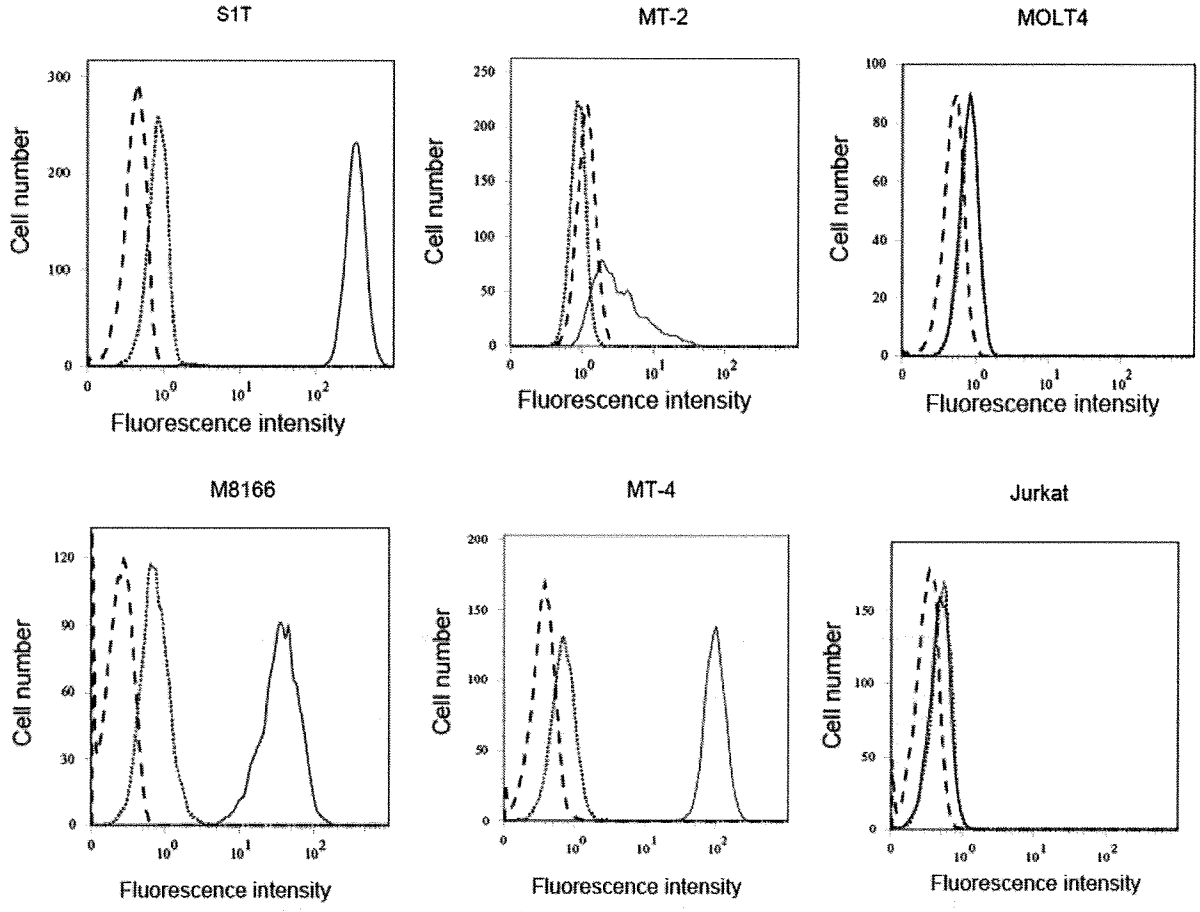

Fig. 4. **Bindings of S1T-A3 scFv to HTLV-1-carrying T-cell lines (S1T, MT-2, MT-4 and M8166) and non-HTLV-1-carrying T-cell lines (MOLT4 and Jurkat).** The cells were stained with scFv, anti-His-tagged mouse mAb and FITC-labelled anti mouse antibody and supplied to FACS analysis (thick line). The broken and dotted lines indicate the cells only and the cells stained without scFv, respectively. The increase of the fluorescence intensity of the cells by binding with scFv was evaluated as the relative mean fluorescence (RMF) with scFv *vs.* without scFv, which gave the values of 330, 116, 51, 3.0, 1.1, 1.2 for S1T, MT-4, M8166, MT-2, MOLT4 and Jurkat cells, respectively.

streptavidin (Beckman Coulter Inc.). The scFv that bound to the cells was stained with an anti-His tag mAb (GE Healthcare) and FITC-conjugated anti-mouse IgG antibody. For staining HLA-DR, PE-conjugated anti-HLA-DR (L243) mAb was used. Cells were washed twice with FACS buffer and then analysed on an EPICS XL flow cytometer (Beckman Coulter Inc.).

Purification of scFv for Cellular Assay—The expression of scFv in *E. coli* HB2151 infected with the phage clone S1T was localized in the cytoplasmic fraction. Therefore, the original C-terminal tag (E-tag) of scFv was replaced with a His-tag by recombination of the gene from pCANTAB5E to a pCANTAB6 vector to generate pCANTAB6/S1T-A3 phage. The phage was infected to *E. coli* HB2151 and the S1T-A3 scFv was expressed in HB2151 by induction of 1 mM IPTG at 30°C. The bacterial cells were disrupted by ultrasonication and the supernatant obtained by centrifugation was supplied to affinity purification on His Trap^{TM}HP column (GE Healthcare), according to the manufacturer's instructions. The scFv was further purified on the gel permeation HPLC on Superdex75 (10/300 GL, GE Healthcare) equilibrated with 0.1 M phosphate buffer (pH 7.0).

Mass Spectrometric Analysis for Antigen Determination—The S1T cells were lysed in lysis buffer (pH 7.4, 10 mM Tris–HCl buffer containing 0.5 mM EDTA, 150 mM NaCl, 1% Tween-20, 50 μg/ml DNase I and protein inhibitor cocktail, Sigma–Aldrich) by combination with the ultrasonic disintegrator. The cell lysate was centrifuged and the supernatant was mixed with 2 × SDS sample buffer containing 5% 2-mercaptethanol and subjected to SDS–PAGE on 5–20% gradient gel. The gel was subsequently supplied to western blot analysis to detect the protein band, which was recognized by S1T-A3 scFv. After CBB-staining, the gel fragment including the positive band on western blot was excised, destained and in-gel digested with trypsin. The digested peptides were analysed on LC-MS/MS (Medigenomics, Germany) and their mass spectrum data were analysed by MASCOT search.

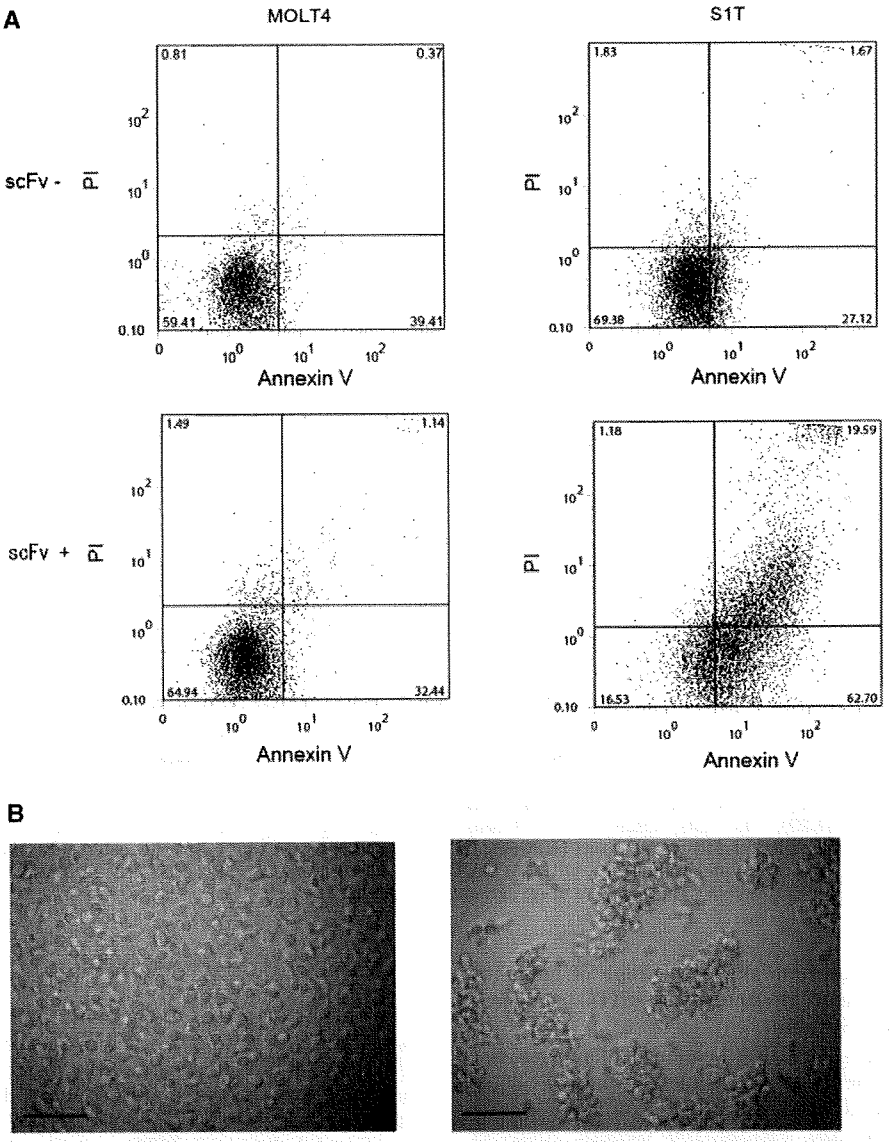

Fig. 5. **Cell death of S1T cells induced by S1T-A3 scFv.** (A) S1T cells or MOLT4 cells were incubated with S1T-A3 scFv (5 nM) at 37°C for 1 h and were stained with propidium iodide (PI) and Annexin V staining solution for 15 min. The stained cells were analysed on a flow cytomer. (B) Morphological aspects of the cell death were examined on OLYMPUS IX71 microscope. The S1T cells were incubated with 10 nM scFv (right panel) or with no scFv (left panel) for 30 min and subjected to the microscopic observation. Scale bar in picture indicates the length of 200 μm.

Preparation of $(scFv)_2$-Fc of SIT-A3—ScFv gene of SIT-A3 was cloned into mammalian expression vector pCAG-H with a human IgG_1 constant region (*16*, pCAG-H- SIT-A3). $(ScFv)_2$-Fc of SIT-A3 was expressed by using FreeStyle 293 system (Invitrogen). Briefly, FreeStyle 293 cells were transfected with a pCAG-H-SIT-A3 by 293 fectin according to the manufacturer's instruction and culture 72 h. The supernatants were removed from the cells by centrifugation and filtered through a 0.22-μm membrane. The expressed $(scFv)_2$-Fc of SIT-A3 was purified by protein A affinity chromatography (GE healthcare). Purified $(scFv)_2$-Fc of SIT-A3 was analysed by size-exclusion chromatography under presence of 0.2 M arginine (*17*).

Cell Killing and Apoptosis Assay—Cells (1×10^5 cell/30 μl) in RPMI 1640 medium containing 10% FBS were incubated with anti-HLA-DR antibodies at 37°C for 30 min. The cells were centrifuged and subjected to the flow cytometer to count the viable cells. The killing activity (%) was evaluated by viable cell recovery: [(viable untreated)–(viable treated)]/(viable untreated) × 100. The Annexin V-FITC assay was also performed

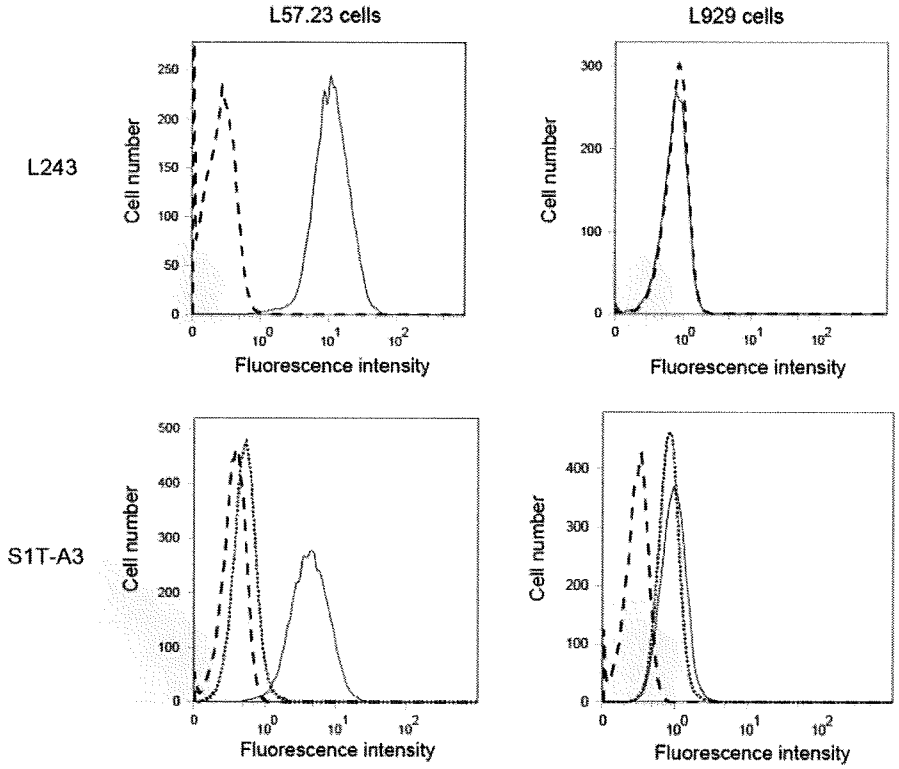

Fig. 6. **Binding specificity of S1T-A3 scFv to HLA-DR-expressing L cells (L57.23).** The cells (L929 or L57.23 cells) were stained with PE-labelled L243 mAb (anti-HLA-αchain mouse mAb, thick line in the upper panel) or with S1T-A3 scFv, anti-His mAb and FITC-labelled anti-mouse mAb (thick line in the lower panel). The dotted lines in the lower panel indicate the data for staining without scFv. The broken lines indicate the data for the cells only. The RMF values of S1T-A3 binding were 9.2 and 1.3 for L57.23 cells and L cells, respectively.

to quantitatively determine the percentage of apoptotic cells using the TACSTM Annexin V-FITC apoptosis detection kit (R&D System).

DNA Sequencing—The DNA sequence of phages was determined by the Dye Terminator method using primer1 (5′-CAACGTGAAAAAATTATTATTCGC-3′ for scFv gene) on the ABI PRISM3100 Genetic Analyzer (Applied Biosystems, Foster City, CA, USA)

ELISA—Each well of the microplate (Nunc, Maxisop) was coated with HLA-DR (50 ng/40 μl/well) in 0.1 M $NaHCO_3$ and blocked with 0.5% BSA in PBS. scFv was added to each well and incubated for 1 h. The wells were washed five times with PBS containing 0.1% Tween-20 and the bound scFv was detected by an anti-His tagged mouse mAb and alkaline-phosphatase (AP)-conjugated anti-mouse IgG (Jackson Immuno Research, West Grove, PA, USA). Using p-nitrophenyl phosphate as a substrate, the colorimetric assay was performed measuring the absorbance at 405 nm using a microplate reader NJ-2300 (System Instruments, Tokyo)

Protein Concentrations—Protein concentrations were determined from the absorbance at 280 nm using molecular extinction coefficients (ε_{280}) of 48,360, 96,720 and 167,400 (absorbance unit of $M^{-1}cm^{-1}$) for scFv monomer, diabody and $(scFv)_2$-Fc, respectively.

RESULTS

Isolation of An Antibody Clone Specific to HTLV-1-Carrying Cells—To isolate a human antibody specific to S1T cells (HTLV-1-carring cells) from a human scFv phage library, the cell panning method in combination with a cell sorter were employed. The S1T cells (1×10^6) were first labelled with FITC-conjugated anti-CD30 mAb, as CD30 is known to be highly expressed by adult T-cell leukaemia cell lines (*18*), mixed with control cells (MOLT4, 1×10^6) and reacted with scFv antibody phage library (1×10^{12} TU). The S1T cells were collected by a cell sorter. The phages binding to the cells were amplified through re-infection to *E. coli* TG1 and supplied to the next round of cell panning. After only two rounds of panning, S1T cells-specific binding phages were enriched (Fig. 1). Among the 30 clones isolated from the pooled phages after the second and third rounds of panning, the 15 clones showed the binding activities to the S1T cells. Their DNA sequences were determined and a single clone S1T-A3 was identified. As shown in Fig. 2, S1T-A3 phage indicated the specific binding to S1T cells with no binding to MOLT4 cells, indicating that S1T-A3 recognized a unique antigen expressed on S1T cell. The amino acid sequences of the VH and VL regions of S1T-A3 are shown in Fig. 3.

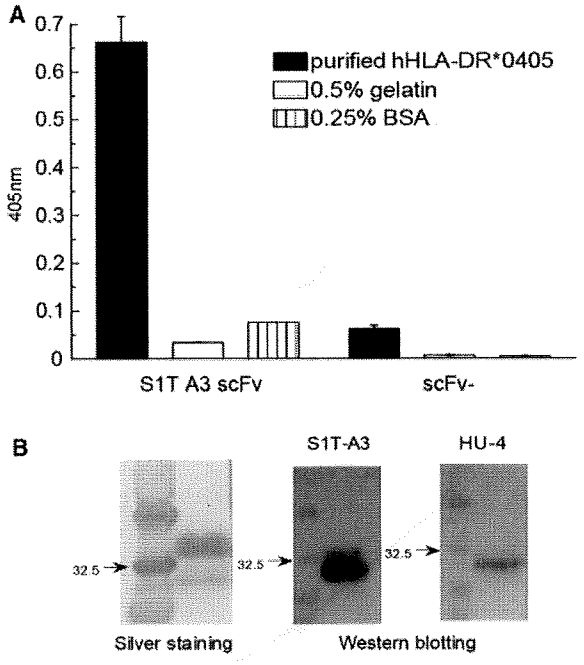

Fig. 7. **Antigen determination of S1T-A3 scFv by ELISA (A) and western blotting (B).** HLA-DR coated on the plate was detected by S1T-A3 scFv, anti-His-tagged mouse mAb and AP-conjugated anti-mouse IgG. The SDS–PAGE gel of HLA-DR was subjected to silver staining or western blot analysis with S1T-A3 scFv or HU-4 mAb (mouse mAb specific to the human HLA-DR β chain). In the silver-stained gel, the upper (34 kDa) and lower (29 kDa) bands corresponded to the HLA-DR α and β chain, respectively.

The scFv was purified from the cytoplasmic fraction of the bacterial cells infected with S1T-A3 phages and the binding analysis was examined against several T cell lymphoma cell lines (HTLV-1-carrying T-cell lines: S1T, MT-2, MT-4 and M8166 and non-HTLV-1-carrying T-cell lines: MOLT4 and Jurkat) on FACS. The results indicated the scFv bound to the four HTLV-1-carring T-cell lines strongly or moderately, but not to the non-HTLV-1-carrying T-cell lines (Fig. 4), suggesting that the cell-surface antigen recognized by S1T-A3 is a potential marker for malignant T-cells during HTLV-1-infection.

Cell-Death-Inducing Activity of S1T-A3 scFv—Of interest, we found that the S1T cells lysed during the incubation with S1T-A3 scFv. Therefore, we examined the apoptotic activity of S1T-A3 by Annexin V/propidium iodide (PI) staining (Fig. 5A). Although apoptosis was generally defined by an increased Annexin V-positive and PI-negative cell population, the S1T cells incubated with S1T-A3 scFv were doubly-stained by PI and Annexin V, suggesting that the cell death induced by S1T-A3 is not typical apoptosis but apoptotic cell death with necrotic properties.

The cell death of S1T cells by S1T-A3 scFv was rapidly induced with 30 min, changing largely the morphology of the cells (Fig. 5B). After incubation of the cells with scFv, the cells were aggregated and lead to cell lysis.

Antigen Targeted by S1T-A3 scFv—We subsequently determined the antigen targeted by S1T-A3 scFv. Western blot analysis of the S1T cell lysate indicated a positive band (32.5 kDa) stained with S1T-A3 scFv (data not shown). The gel fragment corresponding to the positive band on western blot was excised, subjected to in-gel digestion with trypsin and then LC-MS/MS analysis. The mass spectrum data of the obtained peptide fragments were subjected to MASCOT search on human IPI (International Protein Index) database (EMBL-EBI). The potential candidate for antigen of the cell surface was found to be HLA-DRβ.

To confirm this, we examined the binding ability of S1T-A3 scFv to HLA-DR-expressing L57.23 cells, a murine L-cell transfectant with HLA-DRB*0101 and HLA-DRA*0101 genes. S1T-A3 scFv bound to the L57.23 cells but not to control L929 cells (Fig. 6). Furthermore, ELISA and Western blotting analysis using the purified HLA-DR (DRA*0101/DRB1*0405) molecules confirmed the binding of S1T-A3 scFv to HLA-DR and its specificity to β chain of HLA-DR (Fig. 7).

Cell Death Activities Dependent on Molecular Formats of S1T-A3 scFv—Generally, scFv produced by *E. coli* sometimes contains the dimer (diabody) as well as the monomer form. S1T-A3 scFv purified here also contained the two forms of scFv in almost equal amounts, which was detected on the size exclusion chromatography (data not shown). To examine which form is responsible for the cell death activity, each purified scFv form was subjected to cell lysis analysis by counting the viable cells on FACS (Fig. 8). The viable cell number did not change even after treatment with 120 nM scFv monomer. In contrast, the treatment with only 6 nM diabody largely reduced the cell viability to 20%. This finding clearly indicates that the dimer form is essential for the induction of cell death through HLA-DR ligation. This diabody harboured a linker peptide composed of 15 amino acids, $(GGGGS)_3$ between the VH and VL domain. To test the effect of the linker length on cell-death activity, we prepared diabodies with different lengths of linkers composed of $(GGGGS)_2$ and $(GGGGS)_1$, and compared their cell-death activities. The purified three diabodies showed similar dose-dependent activities with EC_{50} of 2–5 nM (data not shown), indicating that the difference of the linker length between 5 and 15 amino acids does not influence the cell death activity so much.

On the other hand, an alternative scFv dimer molecule (a fusion protein of scFv and human IgG Fc, $(scFv)_2$-Fc) was constructed. This molecule showed a comparative binding to S1T cells with a relative mean fluorescence (RMF) of 311 (Fig. 9A), where that of S1T-A3 scFv was 330 (Fig. 4). The surface plasmon resonance (SPR) analysis on BIAcore also showed a tight binding of $(scFv)_2$-Fc to HLA-DR molecules with an apparent dissociation constant K_d of 1.9 nM (Fig. 9B). In spite of its tight binding, $(scFv)_2$-Fc unexpectedly showed a weak cell death-inducing activity (EC_{50}: 26 nM ± 8), which was 15-fold more than that of the diabody (EC_{50}: 1.8 nM ± 0.8) and similar to that of L243 mAb (EC_{50}: 22 nM ± 2), an apoptosis-inducing mouse mAb specific to α chain of HLA-DR.

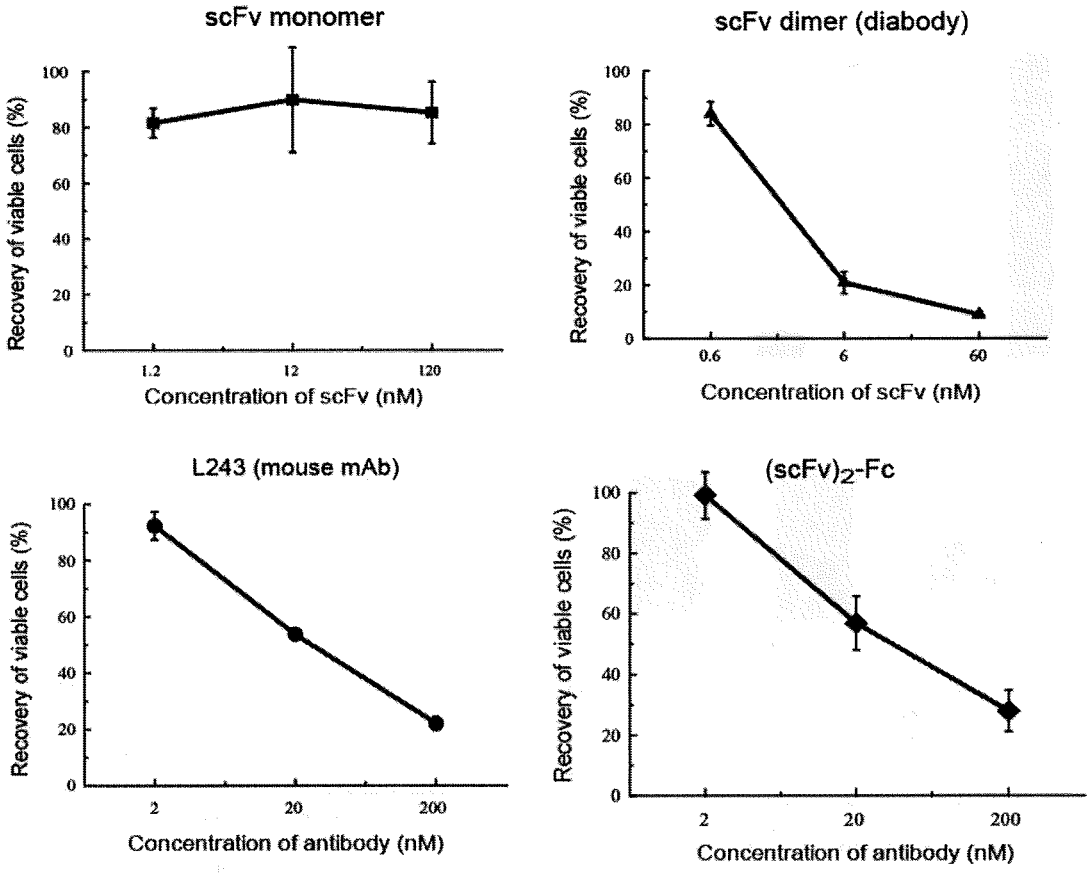

Fig. 8. **Cell-death-inducing activities by the different molecular forms of S1T-A3 scFv [monomer, diabody and $(scFv)_2$-Fc] on S1T cells.** The S1T cells were treated with the different forms of scFv at the indicated concentrations. The viral cells were recovered by centrifugation and were counted using the flow cytometer. The recovery yields of the cells are expressed as a percent ratio of the cell count with *vs.* without the antibody treatment. The L243 mouse mAb was used as a control Ab inducing cell death.

Cell-Death-Inducing Activities of S1T-A3 Diabody on Other HLA-DR Expressing Cells—We further examined the cell-death-inducing activities of S1T-A3 diabody on the cell lines other than S1T cells (Fig. 10A). Under the condition where more than 90% S1T cells died, the cell death was observed in 60% of MT-4, 8% of M8166 and 15% of Daudi cells, and the no significant cell death was done in MOLT4 cells. These cell-death capabilities seem to accord with the expression level of HLA-DR on the surface of the cells. Figure 10B showed the expression level of HLA-DR examined on FACS by staining with anti-HLA-DR α chain mouse mAb (L243). The S1T cells highly expressed HLA (RMF: 520), MT-4 or Daudi cells moderately (RMF: 72, 55). M8166 and MOLT4 cells at very low level or not at all (RMF: 4.0 and 1.0). Interestingly, in spite of the similar expression of HLA (RMF:72 and 55) and the comparable cell-death induction by L243 mAb (14 and 20%) between MT-4 and Daudi cells, the extent of the cell death by S1T-A3 diabody was largely different (15% and 60% for MT-4 and Daudi). This discrepancy may be caused by the differences of the accessory molecules for HLA-derived cell-death signalling and/or of HLA β chain isoforms between the cell lines.

DISCUSSION

In this report, we identified HLA-II molecules as a S1T cell-specific marker by isolation of S1T-specific antibody (scFv) and determination of its antigen. HLA-II (human MHC-class II molecules) is a heterodimer composed of an α chain and a highly variable β chain, and classified into three groups of the gene family, namely HLA-DP, HLA-DQ and HLA-DR. This molecule is expressed on the antigen presenting cells (APC) such as macrophages and dendritic cells, and functions as antigen presentation molecule to T cells in the activation of the immune response (*19*, *20*). It is well known that the expression of these molecules is increased in the malignant lymphomas and therefore especially HLA-DR has become a clinical target for antibody therapy to B-cell lymphoma (*21*, *22*). On the other hand, it was reported that HLA-DR expression is enhanced in the activated T-cells or in malignant T-cells including several

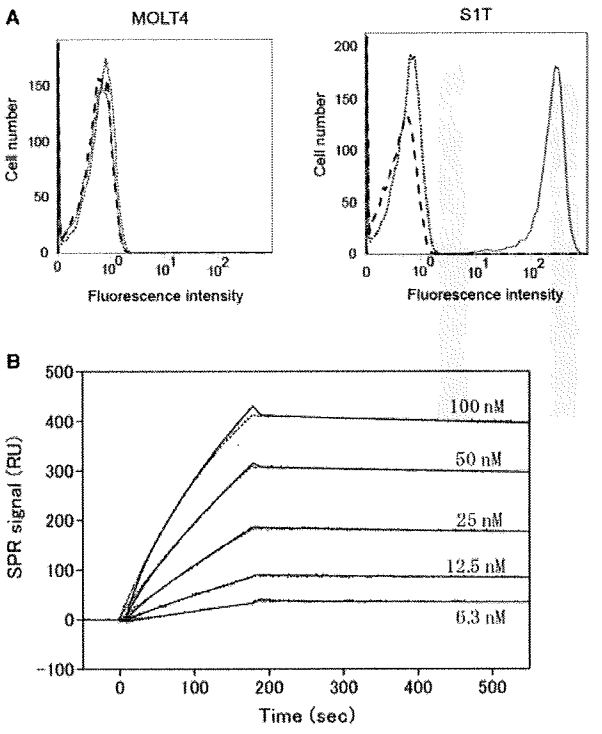

Fig. 9. **Binding analysis of S1T-A3 $(scFv)_2$-Fc to S1T cells on FACS (A) and to HLA-DR molecules by surface plasmon resonance (SPR) analysis (B).** The cells were stained with $(scFv)_2$-Fc, biotinylated anti-human Fc mAb and PE-labelled streptavidin (SA) (thick line). The dotted and broken lines indicate the data for staining without $(scFv)_2$-Fc and the cells only. The relative mean fluorescence (RMF) values of $(scFv)_2$-Fc to S1T and MOLT4 were 311 and 0.8, respectively. SPR analysis was performed on BIAcore 2000 (GE Healthcare) at 25°C and a flow rate of 20 µl/min. The HLA-DR molecules were conjugated to a CM5 sensorchip by the amine-coupling method. The $(scFv)_2$-Fc solution was injected to the flow cells at the indicated concentrations to monitor the association phase and the subsequent dissociation phase by eluting with the running buffer. The kinetic parameters of the binding were evaluated on BIAevaluation 3.2 software assuming a 1:1 binding model to give a dissociation equilibrium constant, K_d of 1.9 nM (k_a, association rate constant: $5.2 \times 10^4\ M^{-1}s^{-1}$, K_d, dissociation constant: $9.6 \times 10^{-5}\ s^{-1}$). The simulation curves calculated on the basis of these parameters were indicated in the dotted lines.

ATL cells (*13, 23*). We demonstrated here that HLA-DR could be a candidate of clinical target for antibody therapy to ATL and that anti-HLA-DR antibody can work effectively to induce the cell death to ATL cell lines in addition to B-cell lymphoma, although its cell killing activity is largely dependent on the expression level of HLA-DR on the cells (Fig. 10).

1D10 (Hu1D10), a human IgG4 antibody isolated from the synthetic human antibody phage library (HuCal) induces apoptosis by a caspase-independent pathway without the aid of effector cells (*21*). However, as described by van der Neut Kolfschoten *et al.* (*24*) as IgG4 antibodies exchange Fab arms by swapping a heavy chain and attached light chain with a heavy-light chain pair from another molecule, such swapping mechanism might reduce efficacy of 1D10. Anti-HLA-DR human antibody HD8 generated by transchromo mouse technology also exhibited cell cytotoxic activity through the effecter cells or the complement (*22*). Other antibodies were used for killing malignant lymphocytes by exerting anti-tumour activity through cell-death signalling (*21, 22, 25–27*).

As compared with these whole antibodies, small fragment antibodies like scFv or minibodies are considered to have several advantages in clinical applications. These include easy control of serum concentration owing to their short half-life in serum, high penetration into target tissues owing to their small sizes, low cost of production using bacterial cells and less side-effects such as antibody (Fc)- or complement-dependent cytotoxicity against the normal cells. Kimura *et al.* (*28*) described a diabody with agonistic activity to induce apoptosis through the ligation of MHC class I molecules by a caspase-independent pathway. This diabody (2D7) showed a 4-fold stronger apoptotic activity on ARH-77 cells (a myeloma cell line) than the original whole antibody 2D7 dimerized by anti-mouse Fc Ab. In our case, the S1T-A3 diabody specific to MHC class II molecules also had 15-fold higher cell-death activity than the $(scFv)_2$-Fc or L243 mouse whole antibody (Fig. 8). These results suggest that the death signalling through MHC class I or II molecules is more effectively exerted by the diabody form rather than by the whole antibody or the $(scFv)_2$-Fc form.

The features of the cell death induced by the S1T-A3 diabody were characterized by PI- and Annexin V- double positive staining on FACS analysis (Fig. 5), which indicates not a typical apoptosis but apoptosis-like cell death with necrotic feature. The similar properties of the cell death by HLA-DR signalling were reported in B-cell lymphoma characterized by caspase-independent pathway (*21*) with accompanying DNA fragmentation (*29*). Recently, Carlo-Stella *et al.* (*30*) proposed another cell-death pathway. The humanized anti-HLA-DR antibody 1D09C3 exerts a potent anti-tumour effect on the chronic lymphocytic leukaemia JVM-2 and the mantle-cell lymphoma cell line GRANTA-519 by activating reactive oxygen species-dependent, c-Jun-NH2-kinase (JNK)-driven cell death. The other paper described that the HLA-DR/CD18 complex stimulated by L243 mAb ligation delivers the cell death signalling through the activation of protein kinase C (PKC) β which is located in the outside of the lipid raft of the cell surface (*31*). Thus, several papers as for signalling pathway of cell death through HLA-DR reported somewhat contradictory results. S1T-A3 diabody exerting an effective anti-tumour activity by a strong cell death may contribute to understanding the cell-death-signalling pathway through HLA-DR.

Based on the earlier findings that CCR4 expression is associated with ATLL (Adult T-cell leukaemia/lymphoma) at a high frequency (88%) (*32*), an anti-CCR4 Ab is under development for ATL treatment (*33*). When using therapeutic agents, which target a single pathogenic marker of the tumour, the appearance of relapses or refractory tumours is problematic. In fact, despite the clinical success of rituximab (anti CD20 mAb), relapse of CD20-negative tumours have been

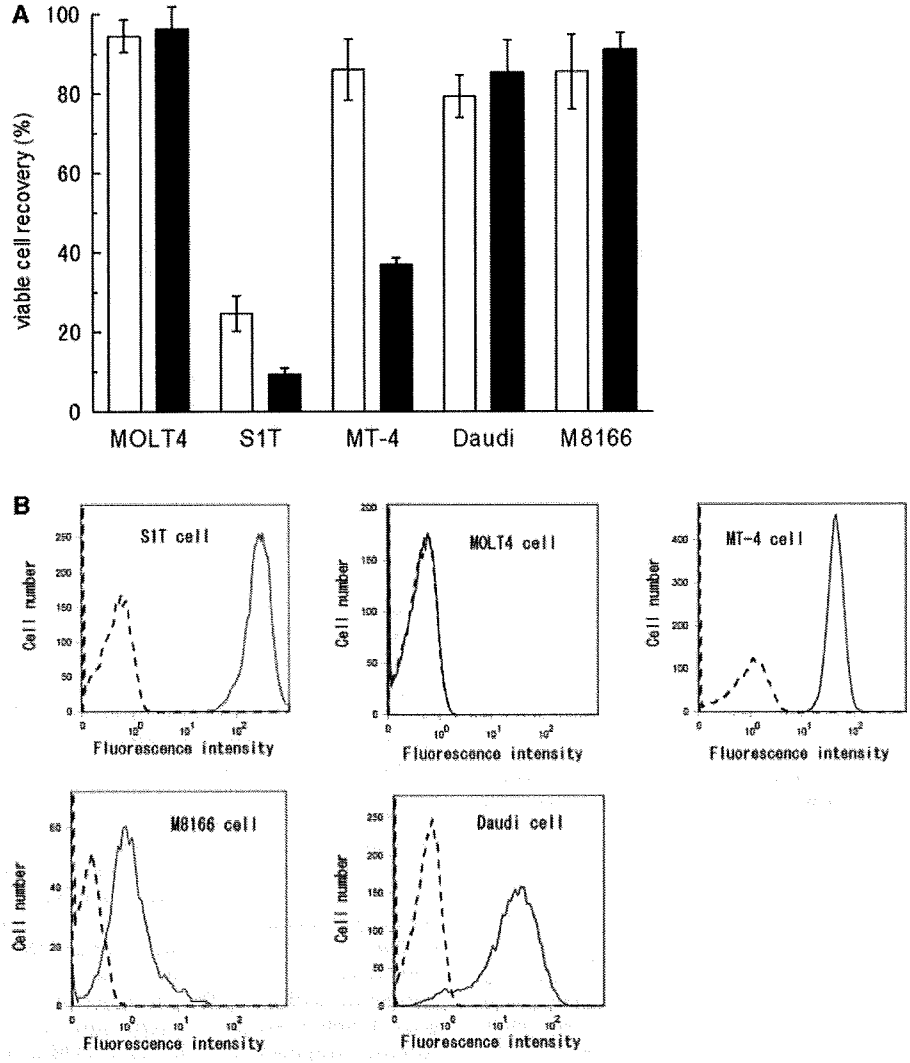

Fig. 10. **Cell-death-inducing activities of S1T-A3 diabody on S1T, MOLT4, Daudi and M8166 and MT-4 cell lines (A) and the expression levels of HLA-II molecules on each cell (B).** The open and filled bars in (A) indicate the viable cell recovery (%) of each cell lines treated with anti HLA-DR α chain mAb L243 (200 nM) and S1T-A3 diabody (60 nM), respectively. S1T-A3 diabody used here are the scFv dimer with GGGGS linker. The expression of HLA molecules in (B) was analysed by staining with L243mAb on FACS. The relative mean fluorescence (RMF) of S1T, MT-4, MOLT4, M8166 and Daudi cells were estimated to be 520, 72, 1.0, 4.0 and 55 respectively.

reported (*34*). Recently, we reported that CD70 is a promising tumour marker for ATL (*13*). We are expecting the anti-HLA-DR diabody to provide an alternative candidate for antibody therapy for ATL with a distinct targets and mechanism of action, together with the anti-CCR4 and anti-CD70 antibodies.

FUNDING

A grant from the Frontier Science Research Center, Kagoshima University; a grant from Japan Science and Technology Agency; and a Grant-in-Aid for Scientific Research (B) from the Japan Society for the Promotion of Science (grant no. 19390153).

CONFLICT OF INTEREST

None declared.

REFERENCES

1. Matsuoka, M. and Jeang, K.T. (2005) Human T-cell leukemia virus type I at age 25: a progress report. *Cancer Res.* **65**, 4467–4470
2. Ohshima, K. (2007) Pathological features of diseases associated with human T-cell leukemia virus type I. *Cancer Sci.* **98**, 772–778
3. Hoogenboom, H.R. (2005) Selecting and screening recombinant antibody libraries. *Nat. Biotechnol.* **23**, 1105–1116
4. Jakobovits, A., Amado, R.G., Yang, X., Roskos, L., and Schwab, G. (2007) From XenoMouse technology to

panitumumab, the first fully human antibody product from transgenic mice. *Nat. Biotechnol.* **25**, 1134–1143
5. Ridgway, J.B., Ng, E., Kern, J.A., Lee, J., Brush, J., Goddard, A., and Carter, P. (1999) Identification of a human anti-CD55 single-chain Fv by subtractive panning of a phage library using tumor and nontumor cell lines. *Cancer Res.* **59**, 2718–2723
6. McWhirter, J.R., Kretz-Rommel, A., Saven, A., Maruyama, T., Potter, K.N., Mockridge, C.I., Ravey, E.P., Qin, F., and Bowdish, K.S. (2006) Antibodies selected from combinatorial libraries block a tumor antigen that plays a key role in immunomodulation. *Proc. Natl Acad. Sci. USA.* **103**, 1041–1046
7. Giordano, R.J., Cardo-Vila, M., Lahdenranta, J., Pasqualini, R., and Arap, W. (2001) Biopanning and rapid analysis of selective interactive ligands. *Nat. Med.* **7**, 1249–1253
8. de Kruif, J., Terstappen, L., Boel, E., and Logtenberg, T. (1995) Rapid selection of cell subpopulation-specific human monoclonal antibodies from a synthetic phage antibody library. *Proc. Natl Acad. Sci. USA* **92**, 3938–3942
9. Watters, J.M., Telleman, P., and Junghans, R. P. (1997) An optimized method for cell-based phage display panning. *Immunotechnology* **3**, 21–29
10. Mutuberria, R., Satijn, S., Huijbers, A., Van Der Linden, E., Lichtenbeld, H., Chames, P., Arends, J.W., and Hoogenboom, H.R. (2004) Isolation of human antibodies to tumor-associated endothelial cell markers by in vitro human endothelial cell selection with phage display libraries. *J. Immunol. Methods* **287**, 31–47
11. Roovers, R.C., van der Linden, E., de Bruine, A.P., Arends, J.W., and Hoogenboom, H.R. (2001) Identification of colon tumour-associated antigens by phage antibody selections on primary colorectal carcinoma. *Eur. J. Cancer* **37**, 542–549
12. Sakaki, Y., Terashi, K., Yamaguchi, A., Kawamata, N., Tokito, Y., Mori, H., Umehara, M., Yoshiyama, T., Ohtsubo, H., Arimura, K., Arima, N., and Tei, C. (2002) Human T-cell lymphotropic virus type I Tax activates lung resistance-related protein expression in leukemic clones established from an adult T-cell leukemia patient. *Exp. Hematol.* **30**, 340–345
13. Baba, M., Okamoto, M., Hamasaki, T., Horai, S., Wang, X., Ito, Y., Suda, Y., and Arima, N. (2008) Highly enhanced expression of CD70 on human T-lymphotropic virus type 1-carrying T-cell lines and adult T-cell leukemia cells. *J. Virol.* **82**, 3843–3852
14. Hashiguchi, S., Nakashima, T., Nitani, A., Yoshihara, T., Yoshinaga, K., Ito, Y., Maeda, Y., and Sugimura, K. (2003) Human Fc epsilon RIalpha-specific human single-chain Fv (scFv) antibody with antagonistic activity toward IgE/Fc epsilon RIalpha-binding. *J. Biochem.* **133**, 43–49
15. Hamasaki, T., Hashiguchi, S., Ito, Y., Kato, Z., Nakanishi, K., Nakashima, T., and Sugimura, K. (2005) Human anti-human IL-18 antibody recognizing the IL-18-binding site 3 with IL-18 signaling blocking activity. *J. Biochem.* **138**, 433–442
16. Maeda, H., Matsushita, S., Eda, Y., Kimachi, K., Tokiyoshi, S., and Bendig, M.M. (1991) Construction of reshaped human antibodies with HIV-neutralizing activity. *Hum. Anitibodies Hybridomas* **2**, 124–134
17. Arakawa, T., Philo, J.S., Ejima, D., Tsumoto, K., and Arisaka, F. (2006) Aggregation Analysis of Therapeutic Proteins, Part 1. *Gen. Asp. Tech. Assess. BioProcess Int.* **4**, 32–43
18. Higuchi, M., Matsuda, T., Mori, N., Yamada, Y., Horie, R., Watanabe, T., Takahashi, M., Oie, M., and Fujii, M. (2005) Elevated expression of CD30 in adult T-cell leukemia cell lines: possible role in constitutive NF-kappaB activation. *Retrovirology* **2**, 29
19. Lang, P., Stolpa, J.C., Freiberg, B.A., Crawford, F., Kappler, J., Kupfer, A., and Cambier, J.C. (2001) TCR-induced transmembrane signaling by peptide/MHC class II via associated Ig-alpha/beta dimers. *Science* **291**, 1537–1540
20. Trautmann, A. and Valitutti, S. (2003) The diversity of immunological synapses. *Curr. Opin. Immunol.* **15**, 249–254
21. Nagy, Z.A., Hubner, B., Lohning, C., Rauchenberger, R., Reiffert, S., Thomassen-Wolf, E., Zahn, S., Leyer, S., Schier, E. M., Zahradnik, A., Brunner, C., Lobenwein, K., Rattel, B., Stanglmaier, M., Hallek, M., Wing, M., Anderson, S., Dunn, M., Kretzschmar, T., and Tesar, M. (2002) Fully human, HLA-DR-specific monoclonal antibodies efficiently induce programmed death of malignant lymphoid cells. *Nat. Med.* **8**, 801–807
22. Tawara, T., Hasegawa, K., Sugiura, Y., Tahara, T., Ishida, I., and Kataoka, S. (2007) Fully human antibody exhibits pan-human leukocyte antigen-DR recognition and high in vitro/vivo efficacy against human leukocyte antigen-DR-positive lymphomas. *Cancer Sci.* **98**, 921–928
23. Shirono, K., Hattori, T., Hata, H., Nishimura, H., and Takatsuki, K. (1989) Profiles of expression of activated cell antigens on peripheral blood and lymph node cells from different clinical stages of adult T-cell leukemia. *Blood* **73**, 1664–1671
24. van der Neut Kolfschoten, M., Schuurman, J., Losen, M., Bleeker, W.K., Martinez-Martinez, P., Vermeulen, E., den Bleker, T.H., Wiegman, L., Vink, T., Aarden, L.A., De Baets, M.H., van de Winkel, J.G., Aalberse, R.C., and Parren, P.W. (2007) Anti-inflammatory activity of human IgG4 antibodies by dynamic Fab arm exchange. *Science* **317**, 1554–1557
25. Bertho, N., Blancheteau, V.M., Setterblad, N., Laupeze, B., Lord, J.M., Drenou, B., Amiot, L., Charron, D.J., Fauchet, R., and Mooney, N. (2002) MHC class II-mediated apoptosis of mature dendritic cells proceeds by activation of the protein kinase C-delta isoenzyme. *Int. Immunol.* **14**, 935–942
26. Shan, D., Ledbetter, J.A., and Press, O.W. (2000) Signaling events involved in anti-CD20-induced apoptosis of malignant human B cells. *Cancer Immunol. Immunother.* **48**, 673–683
27. Ghetie, M.A., Podar, E.M., Ilgen, A., Gordon, B.E., Uhr, J.W., and Vitetta, E.S. (1997) Homodimerization of tumor-reactive monoclonal antibodies markedly increases their ability to induce growth arrest or apoptosis of tumor cells. *Proc. Natl Acad. Sci. USA* **94**, 7509–7514
28. Kimura, N., Kawai, S., Kinoshita, Y., Ishiguro, T., Azuma, Y., Ozaki, S., Abe, M., Sugimoto, M., Hirata, Y., Orita, T., Okabe, H., Matsumoto, T., and Tsuchiya, M. (2004) 2D7 diabody bound to the alpha2 domain of HLA class I efficiently induces caspase-independent cell death against malignant and activated lymphoid cells. *Biochem. Biophy.s Res. Commun.* **325**, 1201–1209
29. Drenou, B., Blancheteau, V., Burgess, D.H., Fauchet, R., Charron, D.J., and Mooney, N. A. (1999) A caspase-independent pathway of MHC class II antigen-mediated apoptosis of human B lymphocytes. *J. Immunol.* **163**, 4115–4124
30. Carlo-Stella, C., Di Nicola, M., Turco, M. C., Cleris, L., Lavazza, C., Longoni, P., Milanesi, M., Magni, M., Ammirante, M., Leone, A., Nagy, Z., Gioffre, W.R., Formelli, F., and Gianni, A.M. (2006) The anti-human leukocyte antigen-DR monoclonal antibody 1D09C3 activates the mitochondrial cell death pathway and exerts a potent antitumor activity in lymphoma-bearing nonobese diabetic/severe combined immunodeficient mice. *Cancer Res.* **66**, 1799–1808
31. Doisne, J.M., Castaigne, J.G., Deruyffelaere, C., Dieu-Nosjean, M.C., Chamot, C., Alcaide-Loridan, C., Charron, D., and Al-Daccak, R. (2008) The context of HLA-DR/CD18 complex in the plasma membrane governs

HLA-DR-derived signals in activated monocytes. *Mol. Immunol.* **45**, 709–718
32. Ishida, T., Inagaki, H., Utsunomiya, A., Takatsuka, Y., Komatsu, H., Iida, S., Takeuchi, G., Eimoto, T., Nakamura, S., and Ueda, R. (2004) CXC chemokine receptor 3 and CC chemokine receptor 4 expression in T-cell and NK-cell lymphomas with special reference to clinicopathological significance for peripheral T-cell lymphoma, unspecified. *Clin Cancer Res.* **10**, 5494–5500
33. Murata, K. and Yamada, Y. (2007) The state of the art in the pathogenesis of ATL and new potential targets associated with HTLV-1 and ATL. *Int. Rev. Immunol.* **26**, 249–268
34. Jazirehi, A.R. and Bonavida, B. (2005) Cellular and molecular signal transduction pathways modulated by rituximab (rituxan, anti-CD20 mAb) in non-Hodgkin's lymphoma: implications in chemosensitization and therapeutic intervention. *Oncogene* **24**, 2121–2143
35. Brochet, X., Lefranc, M P., and Giudicelli, V. (2008) IMGT/V-QUEST: the highly customized and integrated system for IG and TR standardized V-J and V-D-J sequence analysis. *Nucleic Acids Res.* **36**, W503–W508

J. Biochem. 2009;146(1)33–41
doi:10.1093/jb/mvp041

High-Sensitivity Analysis of Naturally Occurring Sugar Chains, Using a Novel Fluorescent Linker Molecule

Masaki Sato[1], Yuji Ito[2], Naomichi Arima[3], Masanori Baba[3], Michael Sobel[4], Masahiro Wakao[1] and Yasuo Suda[1,5,*]

[1]Department of Nanostructure and Advanced Materials; [2]Department of Bioengineering, Graduate School of Science and Engineering, Kagoshima University, 1-21-40, Kohrimoto, Kagoshima 890-0065; [3]Center for Chronic Viral Diseases, Graduate School of Medical and Dental Sciences, Kagoshima University, Japan; [4]Department of Surgery, VA Puget Sound HCS and The University of Washington School of Medicine, Seattle, WA, USA; and [5]SUDx-Biotec Corp., 1-42-1, Shiroyama, Kagoshima, 890-0013, Japan

Received February 16, 2009; accepted February 26, 2009; published online March 6, 2009

To analyse the binding of sugar chains to proteins, viruses and cells, the surface plasmon resonance (SPR) technique is very convenient and effective because it is a real-time, non-destructive detection system. Key to this method is linker compounds for immobilization of the sugar chains to the gold-coated chip for SPR. Also, well-designed fluorescent labelling reagents are essential when analysing the structure of trace amounts of sugar chains derived from natural sources, such as glycoproteins on the surface of specific cells. In this report, we developed a novel linker molecule, named 'f-mono', which has both of these properties: simple immobilization chemistry and a fluorescent label. Since the molecule contains a 2,5-diaminopyridyl group and a thioctic acid group, conjugation with sugar chains can be achieved using the well-established reductive amination reaction. This conjugate of sugar chain and fluorescent linker (fluorescent ligand-conjugate, FLC) has fluorescent properties (ex. 335 nm, em. 380 nm), and as little as 1 μg of FLC can be easily purified using HPLC with a fluorescent detector. MS and MS/MS analysis of the FLC is also possible. As a +2 Da larger MS peak ($[M+H+2]^+$ ion) was always associated with the theoretical MS peak ($[M+H]^+$) (due to the reduction of the thioctic acid moiety), the MS peaks of the FLC were easily found, even using unfractionated crude samples. Immobilization of the FLC onto gold-coated chips, and their subsequent SPR analyses were successively accomplished, as had been performed previously using non-fluorescent ligand conjugates.

Key words: immobilization, sugar chain, high sensitivity, analysis, fluorescence, linker molecule, mass spectrometry.

Abbreviations: DMAc, N, N-dimethyl acetoamide; aoWS, N^{α}-((aminooxy)acetyl)tryptophanylarginine methyl ester.

The carbohydrates that make up proteoglycans, glycoproteins or glycolipids are responsible for many biological functions and play crucial roles in cellular binding and signalling (*1*). However, because of their structural complexity, the methods for studying sugar chains are more challenging than that for DNA, RNA or proteins. The numerous isomeric and anomeric configurations of sugar chains, as well as the difficulties in isolating sufficient quantities of naturally occurring sugars, make binding analysis and structure–function studies challenging.

For the structural analysis of naturally occurring sugar chains, fluorescent labelling of the sugars has been one popular technique (*2*). Recently, mass spectrometry (MS) has been used for structural analysis of sugar structures, thanks to the development of structurally well-defined standards (*3*, *4*). Surface plasmon resonance (SPR) methodology is also a very effective method to quantify binding interactions between sugar-chains and lectins or viruses in real time, because it is a non-destructive technology that does not require large quantities of the often scarce materials to be studied (*5–9*). We have previously reported the development of the 'sugar chip', in which defined sugar chains are immobilized on an SPR sensor chip using our specialized linker molecules (*10*, *11*). But the purification of these linker-carbohydrate conjugates for SPR has been difficult when the quantities of the target sugar chains were limited (*i.e.* <1 mg). To overcome this and the other challenges in the analysis of scarce sugar chains, we have developed a novel carbohydrate linker molecule that is also fluorescent (named 'f-mono'). Here we report the successful synthesis of this novel fluorescent linker molecule, and the preparation and purification of conjugates (fluorescent ligand-conjugate or FLC) using as little as 1 μg of sugar chain. These FLCs were then effectively employed in SPR analysis of carbohydrate–protein binding, as well as MS and MS/MS structural analyses.

MATERIALS AND METHODS

General Procedure—All reactions in organic media were carried out with freshly distilled solvents or with

*To whom correspondence should be addressed. Tel: +81-99-285-8369, Fax: +81-99-285-8369, E-mail: ysuda@eng.kagoshima-u.ac.jp

commercially available extra grade solvents purchased from Kanto Chem. Co. (Tokyo, Japan), Nacalai Tesque (Kyoto, Japan) or Wako Chem. Co. (Osaka, Japan). Silica gel column chromatography was performed using PSQ 60B (Fuji Silysia Chem. Ltd., Aichi, Japan). Electrospray ionization time-of-flight mass (ESI-TOF/MS) spectra were obtained by Mariner™ (Applied Biosystems, Framingham, MA, USA). ^{1}H-NMR measurements were performed with JEOL (Tokyo, Japan) ECA-600.

Synthesis of f-mono linker—2,6-Diaminopyridine (1.06 g, 9.70 mmol, Sigma, USA) and thioctic acid (1.00 g, 4.80 mmol, Sigma, USA) were dissolved in anhydrous *N, N*-dimethylformamide (10 ml). Then, 1-hydroxy-7-azabenzotriazole (HOAt, 0.66 g, 4.80 mmol), 1-ethyl-3-(3-dimethylaminopropyl)carbodiimide monohydrochloride (EDC-HCl, 0.93 g, 4.80 mmol), and diisopropylethylamine (DIEA, 0.84 ml, 4.80 mmol) were added to the solution. After stirring for 6 h under argon gas, the reaction product was extracted into the organic phase using dichloromethane (CH_2Cl_2, 20 ml), and was washed with water (10 ml) three times and then with saturated sodium bicarbonate aqueous solution. The product was then purified by silica gel column chromatography (80 g, eluted with toluene/ethyl acetate = 3/1, v/v) to obtain a yellow solid. Yield: 1.37 g (95%). MS calcd. for $C_{13}H_{19}N_3OS_2$: 297.10, Found: *m/z* 298.12 $[M+H]^+$; ^{1}H NMR (600 MHz, CDCl3), δ7.58 (1H, s), 7.53 (1H, d, J = 7.5 Hz), 7.46 (1H, t, J = 7.6, J = 8.2 Hz), 6.26 (1H, d, J = 8.2 Hz), 4.24 (1H, m), 3.59–3.56 (1H, m), 3.19–3.10 (2H, m), 2.48–2.44 (1H, m), 2.37–2.34 (2H, m), 1.93–1.90 (1H, m), 1.77–1.68 (4H, m), 1.53–1.48 (2H, m).

Preparation of a Conjugate with Lactose—Lactose monohydrate (20 mg, 56 μmol) and f-mono (18 mg, 61 μmol) were dissolved in a 2.2 ml solution of H_2O/AcOH/DMAc = 5/1/5 (v/v/v). After stirring for 5 h, sodium cyanoborohydrate (17 mg, 280 μmol) was added to the solution. The reaction mixture was left standing at 37°C for 1.5 days and lyophilized. The residue was dissolved in water and purified with an ODS column (20 g, 1.8 cmΦ × 46 cm, eluted with water/methanol = 1/1, v/v). The appropriate fraction was lyophilized with water to obtain the desired final product: fluorescent ligand-conjugate (FLC, abbreviated as Galβ1-4Glc-f-mono) as a white powder. Yield: 19 mg (50%). MS calcd. for $C_{25}H_{41}N_3O_{11}S_2$: 623.17, Found: m/z 624.17 $[M+H]^+$; ^{1}H NMR (600 MHz, MeOD), δ 7.31 (1H, d, J = 8.1 Hz), 6.99 (1H, d, J = 2.0 Hz), 6.20 (1H, d, J = 8.0 Hz), 4.28 (1H, d, H-1′), 3.89 (1H, dd, H-4), 3.75 (2H, m, H-2, H-5), 3.63 (3H, m, H-3, H-6a, H-6b), 3.52 (1H, m), 3.45 (1H, m, H-4′), 3.30 (2H, m, H-3′, H-5′), 3.25–3.14 (2H, m, H-1a,H-2′), 3.05–2.94 (3H, m, H-1b), 2.36 (1H, m), 2.26 (2H, t, J = 7.3 Hz), 1.84–1.76 (1H, m), 1.54–1.35 (6H, m).

Preparation of a Conjugate with Maltose—Maltose (20 mg, 56 μmol) and f-mono (18 mg, 61 μmol) were dissolved in a 2.2 ml solution of H_2O/AcOH/DMAc = 5/1/5 (v/v/v). After stirring for 5 h, sodium cyanoborohydrate (17 mg, 280 μmol) was added to the solution. The reaction mixture was left standing at 37°C for 1.5 days, and lyophilized. The residue was dissolved in water and purified with ODS column (20 g, 1.8 cmΦ × 46 cm, eluted with water/methanol = 1/1, v/v). The appropriate fraction was lyophilized with water to obtain Glcα1-4Glc-f-mono as a white powder. Yield: 17 mg (46%). MS calcd. for $C_{25}H_{41}N_3O_{11}S_2$: 623.17, Found: m/z 624.17 $[M+H]$+; ^{1}H NMR (600 MHz, MeOD), δ 7.32 (1H,d), 6.99 (1H, d), 6.20 (1H, d), 4.95 (1H, s, H-1′), 3.89–3.78 (3H, m, H-2, H-4, H-5), 3.63 (3H, m, H-3, H-6a, H-6b), 3.42 (1H, m), 3.38 (1H, d, H-4′), 3.13 (2H, m, H-3′, H-5′), 2.85–2.3 (5H, m, H-1a,H-2′), 3.05–2.94 (3H, m, H-1b), 2.36 (1H, m), 1.74–1.26 (7H, m).

SPR Analysis—SPR experiments were perfomed with a 12-channel SPR machine (Moritex Co., Yokohama, Japan) using the manufacturer's recommended guidelines with slight modification. Sensor chips used for SPR experiments were prepared as follows. The gold-coated chip was purchased from SUDx-Biotec (Kagoshima, Japan), and washed in ozone cleaner. The chip was soaked in a 10-, 1-, or 0.1-μM solution of Galβ1-4Glc-f-mono or Glcα1-4Glc-f-mono, dissolved in methanol/water = 1/1 (v/v) at room temperature for 2 h or overnight, followed by subsequent washing with a methanol/water (1/1, v/v) containing 0.05% Tween-20, phosphate-buffered saline (PBS) at pH 7.4 containing 0.05% Tween-20, and PBS (pH 7.4). All washings were done with ultra-sonication for 20 min.

Binding studies were performed between test proteins in the aqueous phase and the stated sugars immobilized via fluorescent linkers (f-mono) attached to the sugar chips. The test proteins concanavalin A (Con A, EY Laboratories, San Mateo, CA, USA), RCA120 (Ricinus Communis Agglutinin I, Vector Laboratories, Servion, Switzerland), and bovine serum albumin (BSA, Nakalai Tesque) were perfused in the aqueous phase (PBS with 0.05% Tween-20 at pH 7.4) at a flow rate of 15 μl/min at 25°C.

Fluorescent Spectra—Fluorescent spectra were measured with a Spectro Fluorometer FP-6310 (JASCO, Tokyo, Japan). The concentration of f-mono was 100 μg/ml in $CHCl_3$. For comparison, our previous mono-valent non-fluorescent linker molecule [abbreviated as 'mono' in this paper (*11*)] was dissolved in $CHCl_3$ at 100 μg/ml, and used as a control.

Mass Spectrometry—MS and MS/MS spectra of FLCs were obtained with an AXIMA-QIT (Shimadzu, Kyoto, Japan), which is a quadrupole ion trap and matrix-assisted laser desorption/ionization time-of-flight mass spectrometer (QIT-MALDI-TOF/MS). Acquisition and data processing were controlled by the manufacturer's software (Kratos Analytical, Manchester, UK). For matrix, a purified 2,5-dihydroxybenzoic acid (DHBA) was dissolved in a mixed solvent with double distilled water containing 0.1% TFA/acetonitrile = 3/1 (v/v) at 10 mg/ml. To 1 μl of sample dissolved in the above mixed solvent spotted on a stainless-steel target, an equal volume of matrix solution was placed and allowed to dry.

Preparation of f-mono-Labelled Glycans from Human IgG—One hundred micrograms of human IgG (Institute of Immunology Co., LTD., Tokyo, Japan) was dissolved in 5 μl of H_2O and 5 μl of 1 M aqueous NH_4HCO_3, and 5 μl of 120 mM aqueous dithiothreitol were added. The reaction solution was heated at 60°C for 30 min. Then, 10 μl of 123 mM aqueous iodoacetamide was added. After incubation in the dark at room temperature for an hour, 10 μl of

trypsin (Sigma-Aldrich, 40 U/μl, dissolved in 1 mM HCl) was added. After an hour, trypsin was inactivated by heating at 90°C for 5 min. Then, 10 U of PNGase F (Roche, Switzerland) was added to the solution (*12*). After incubating at 37°C for 12 h, the solution was lyophilized.

The lyophilized residue was dissolved in 20 μl of H_2O, and concentrated by Blot Glyco (Kit No. MALDI type BS-45601S, Sumitomo Bakelite Co., Ltd. Tokyo, Japan) (*13*, *14*). At the final stage, using the manufacturer's guideline, N-glycans from IgG were released in H_2O, lyophilized and transformed to fluorescent ligand conjugates as follows. The mixture of naturally occurring lyophilized N-glycans and f-mono (100 mg, 340 μmol) were dissolved in 1.0 ml of a mixed solvent (H_2O/AcOH/DMAc = 5/1/5, v/v/v). After 5 h, sodium cyanoborohydrate (62 mg, 1.0 mmol) was added to the solution. The reaction mixture was left standing at 37°C for 1.5 days and lyophilized. To the residue, 200 μl of H_2O was added. Then, the aqueous phase was washed three times with 200 μl of phenol/$CHCl_3$ (1:1, v/v). The aqueous layer was concentrated in vacuo, and excess f-mono and other chemical reagents were removed using an ODS short column attached to the kit. For comparison, the N-glycans of IgG were transformed to the 'sugar-aoWRs condensation product (*15*)' according to the manufacturer's manual. The labelled N-glycans were examined by HPLC (Pump: L-6200, HITACHI, Tokyo, Japan; Detector: FP 2020, JASCO, Tokyo, Japan; Column: COSMOSIL 5C_{18}-PAQ Waters, Nacalai Tesque; Elution: H_2O/MeOH = 1/1, v/v), and by mass spectrometry as described above.

RESULTS AND DISCUSSION

Introducing fluorescence into the linker was accomplished by replacing the 2,6-diaminobenzene unit of our original linker molecule (mono) (*11*), with a 2,6-diaminopyridine moiety (Scheme 1). The labelling of sugar chains using 2-aminopyridine (PA) reported by Hase *et al.* (*16*) was a pioneering advance for the analysis of trace amounts of sugar-chains, and has been applied to 2- or 3-dimensional mapping by Takahashi *et al.* (*17*, *18*) for the conventional structural identification of sugar chains from natural sources, such as glycoproteins. The high fluorescence of the 2,6-diaminopyridine moiety has also been well established, and its use for the biotinylation or immobilization of sugar chains has been reported (*19*, *20*). As expected, our novel f-mono linker molecule showed fluorescence at an excitation (ex) maximum of 335 nm and an emission (em) maximum of 380 nm. Since the sensitivity of detection of fluorescence is about 1,000 times higher than that of UV/VIS, a small quantity (~1 nmol) of sugar chain can be effectively derivatized by using this f-mono linker molecule. In addition, the molecular absorption coefficient (ε value) of f-mono was five times higher than that of the original linker molecule from which it was derived, indicating increased sensitivity even with a standard UV/VIS detector.

Figure 1 shows the SPR data of Con A, RCA120 and BSA binding to α-glucose or β-galactose immobilized *via* FLCs prepared with the f-mono linker to the sensor chip. BSA was used as a negative control, because our previous investigation (*21*) showed that it does not bind to

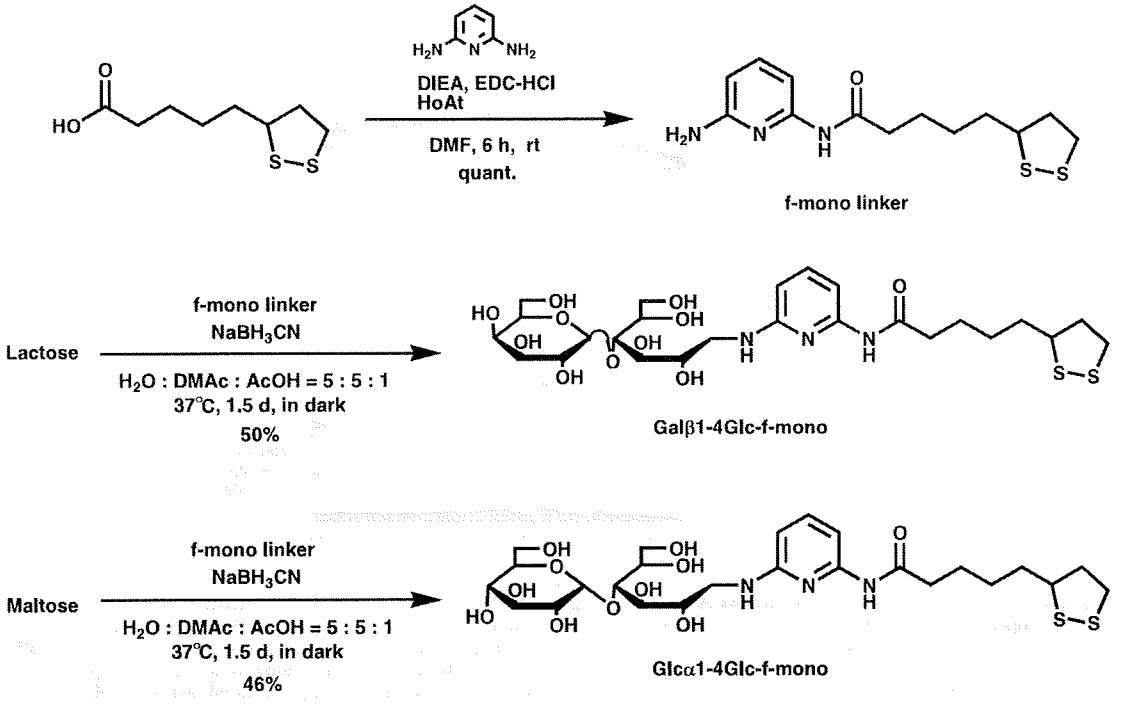

Scheme 1. **Synthesis of f-mono linker and preparation of ligand conjugates, Galβ1-4Glc-f-mono and Glcα1-4Glc-f-mono.**

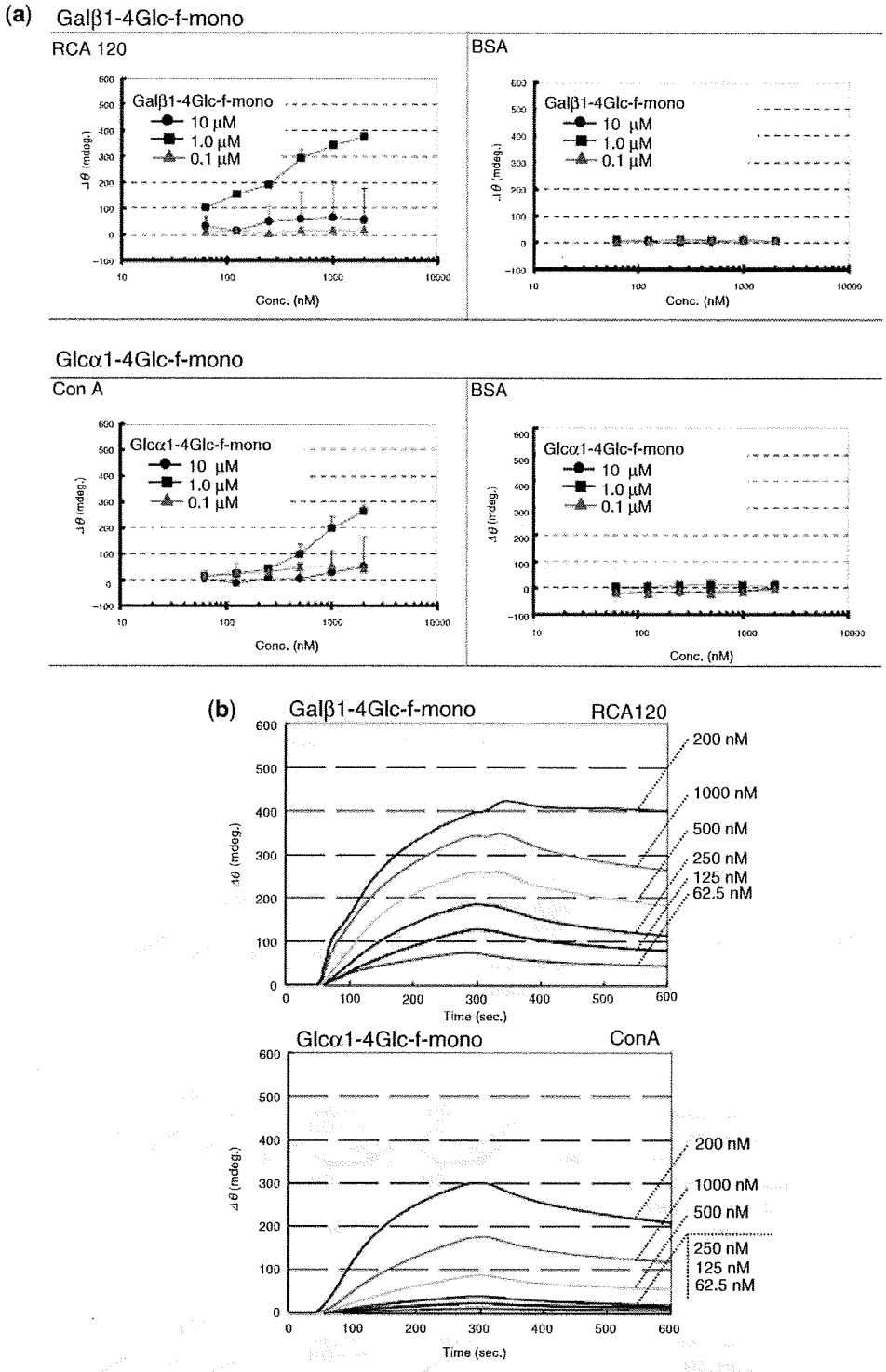

Fig. 1. **SPR analysis of lectins (Con A and RCA120) binding to defined sugars.** Galβ1-4Glc-f-mono or Glcα1-4Glc-f-mono were immobilized on gold-coated chips (see MATERIALS AND METHODS section for details). The test proteins were perfused in the aqueous phase (PBS with 0.05% Tween-20 at pH 7.4) at a flow rate of 15 μl/min at 25°C using a 12-channel SPR machine (Moritex Co., Tokyo, Japan). (a) Dependency of the lectin binding on concentration of FLCs immobilized on the chip. (b) SPR sensor grams of RCA120 for the Galβ1-4Glc-f-mono chip, and Con A for the Glcα1-4Glc-f-mono chip, immobilized at 1 μM.

α-glucose or β-galactose. Figure 1(a) illustrates the dependency of protein binding on the density of immobilization of the sugar chain *via* FLCs on the chip. The data suggest that the optimal density for immobilization of both FLCs appears to be ~1 μM. At higher concentrations, steric hindrance due to the high concentration of ligands may occur and prevent the binding of protein. At 0.1 μM of FLC the ligand sugar chains may be too diluted on the chip to effectively bind protein, because of non-clustered ligands.

Using the chip immobilized with Galβ1-4Glc-f-mono, it was detected that RCA120 bound, but Con A and BSA did not. In contrast, using the chip with Glcα1-4Glc-fmono, Con A bound, but RCA120 and BSA did not. The binding of BSA to the sensor chips was negligible.

Figure 1(b) shows typical sensorgrams of RCA120 and Con A binding to the appropriate sugar chip. The calculated binding parameters were in agreement with those in the literatures (*22*, *23*) and with our previous data using a non-fluorescent linker molecule. The kinetic parameters were; RCA120 *vs.* Galβ1-4Glc-f-mono, $k_{on} = 6.3 \times 10^3\,M^{-1}s^{-1}$, $k_{off} = 4.1 \times 10^{-3}\,s^{-1}$, $K_D = 0.66\,\mu M$; Con A *vs.* Glcα1-4Glc-f-mono, $k_{on} = 2.5 \times 10^3\,M^{-1}s^{-1}$, $k_{off} = 3.1 \times 10^{3}\,s^{-1}$, $K_D = 1.2\,\mu M$.

The results of MS and MS/MS analyses of Galβ1-4Glc-f-mono are shown in Fig. 2. A set of two unique peaks was detected. In addition to the regular $[M+H]^+$ and

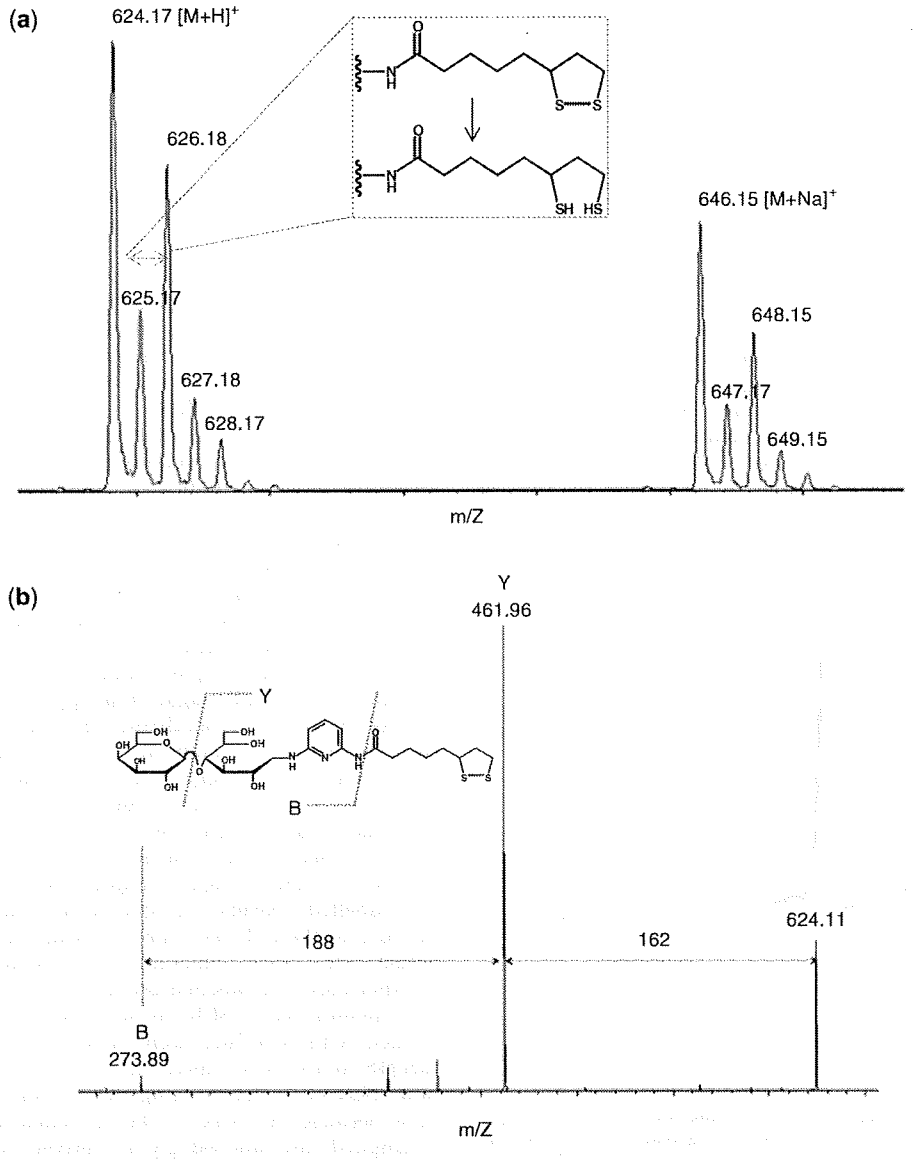

Fig. 2. **MS and MS/MS analyses of Galβ1-4Glc-f-mono.** A quadrupole ion trap and matrix-assisted laser desorption/ionization time-of-flight mass spectrometer (AXIMA-QIT) was used (see MATERIALS AND METHODS section for details). (a) MS spectrum of Galβ1-4Glc-f-mono; (b) MS/MS analysis of Galβ1-4Glc-f-mono.

$[M+Na]^+$ ion, 2-Da bigger peaks ($[M+H+2]^+$ and $[M+Na+2]^+$) were found [Fig. 2(a)]. These later peaks were derived from the reduction of the disulphide bond in the thioctic acid moiety of f-mono, since DHB (the matrix for MALDI) tends to reduce samples with the laser energy (*24*). This property of the f-mono linker was very useful for distinguishing MS peaks of f-mono-labelled glycans from contaminating peaks. In the MS/MS analysis, peaks lacking a galactose unit and thioctic acid from the precursor ion (m/z 624) were observed [Fig. 2(b)]. The cleavage here was as simple in the MS/MS analysis as that using PA-labelled sugar chains (*3*), facilitating structural analysis. For analysing structure and identifying specific sugars, the f-mono linker greatly enhanced the ability to recognize the labelled glycans. From these results, it is suggested that our f-mono linker is a highly effective reagent for MS analysis, at least in a system employing MALDI-QIT and DHBA.

Next, the N-glycans of human IgG were analysed using f-mono. As described in MATERIALS AND METHODS section, N-glycans were extracted from human IgG, concentrated, and then reacted with f-mono. Figure 3 shows the HPLC profile. Two fractions were collected and analysed using MS and MS/MS to confirm f-mono-labelled N-glycans (Fig. S1). From the MS and MS/MS, 162 or 203 different peaks were obtained, suggesting the carbohydrate-derived compounds. In addition, the f-mono labelled glycans were quite easily visualized as +2-Da differentially larger peaks in MS. From the calibration curve (Fig. S2) prepared with Galβ1-4Glc-f-mono, 518 pmol of labelled compounds were estimated to obtain from 100 μg of IgG using the HPLC results, and the detection limit in our HPLC system was estimated to be 5 pmol in 10 μl of injected sample solution.

For comparison, the released N-glycans were also labelled with a reagent (aoWRs) from the kit for MS.

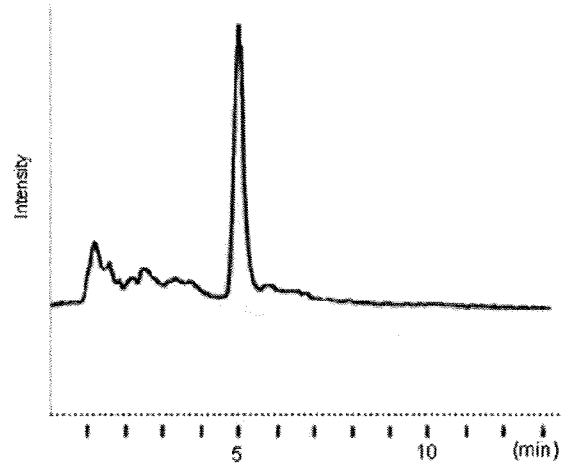

Fig. 3. **HPLC profile of f-mono labelled N-linked sugar chains from IgG.** The extraction of N-glycan and its labelling are described in the MATERIALS AND METHODS section. The conditions of HPLC were as follows. Column: COSMOSIL $5C_{18}$-PAQ Waters (Nacalai Tesque, 4.6 × 150 mm); elution: methanol/water = 1/1 (v/v).

By HPLC analysis, aoWRs-labelled N-glycans did not reveal any detectable peaks because aoWRs had no fluorescence. The MS data are summarized in Fig. 4. The MS spectrum of aoWRs-labelled N-glycans showed six glycan peaks clearly [Fig. 4(a)]. But in the case of the f-mono-labelled glycans, four additional glycans were clearly detected in the MS spectrum [Fig. 4(b)]. Furthermore, the larger 2-Da ions were observed as described above. Figure 4(c) shows the MS/MS spectrum of m/z 1947.1 ions of f-mono-labelled N-glycans. A wealth of structural information could be obtained from this spectrum. For example, from this peak the structure of the glycan containing four hexosamines and five hexoses was easily disclosed. In contrast, the MS/MS analysis of aoWRs-labelled glycan was not possible (data not shown).

The fluorescent intensity of the f-mono reagent was about 1/3 compared to that of 6-aminopyridine (PA) at the same concentration. Therefore, as judged by fluorescent intensity alone, the f-mono reagent is less sensitive. PA-derivatized sugar chains can be analysed by MS, but the f-mono derivatized one can be more easily detected because +2 Da differentially larger peaks are seen every time. Therefore, the novelty of this f-mono reagent is not the improvement of fluorescent sensitivity, but the significant improvement in MS peak identification. Moreover, the derivatized and analysed sugar chain with f-mono can be immobilized on SPR sensor chip sequentially. That is, the extensive merit of this f-mono reagent is that a more-comprehensive and integrated analysis of sugar chains can be sequentially performed using HPLC, MS and SPR.

The difficulty of synthesizing rigorously, structurally defined sugar chains remains a significant challenge to structure–function studies of carbohydrates. Narimatsu and colleagues (*25*) have made important advances in the preparation of sugar-chains using glycosyltransferases, and this synthetic approach holds promise. However, at this time, it is still challenging to prepare large, complex sugar chains. Therefore, for structure–function analyses, approaches that are economical in their use of scarce sugar chains have advantages. One solution is the SPR sugar-chip approach we have illustrated here. By immobilizing the sugar chains on the chip one can use it multiple times. In this case, it is a key to have an efficient linker molecule for immobilization of trace amounts of the defined sugar chain, of which the f-mono linker molecule is a good example.

In conclusion, the f-mono linker molecule is easily synthesized and its ligand-conjugates are easily purified. The labelled glycans are able to be traced with HPLC because of their fluorescence, making this a good application for trace amounts of glycan (~1 pmol/μl). Furthermore, the labelled glycan can be used for binding experiments using SPR, as we have previously demonstrated with non-fluorescent linker-conjugates. MS and MS/MS analyses of f-mono-labelled glycan were possible and effective in determining the glycan's primary structure, because the larger 2-Da ion peaks could be used to distinguish the labelled glycan-derived peaks. With this novel linker molecule, both the structural and functional binding analysis of trace amount of glycans are greatly facilitated, suggesting that this fluorescent linker

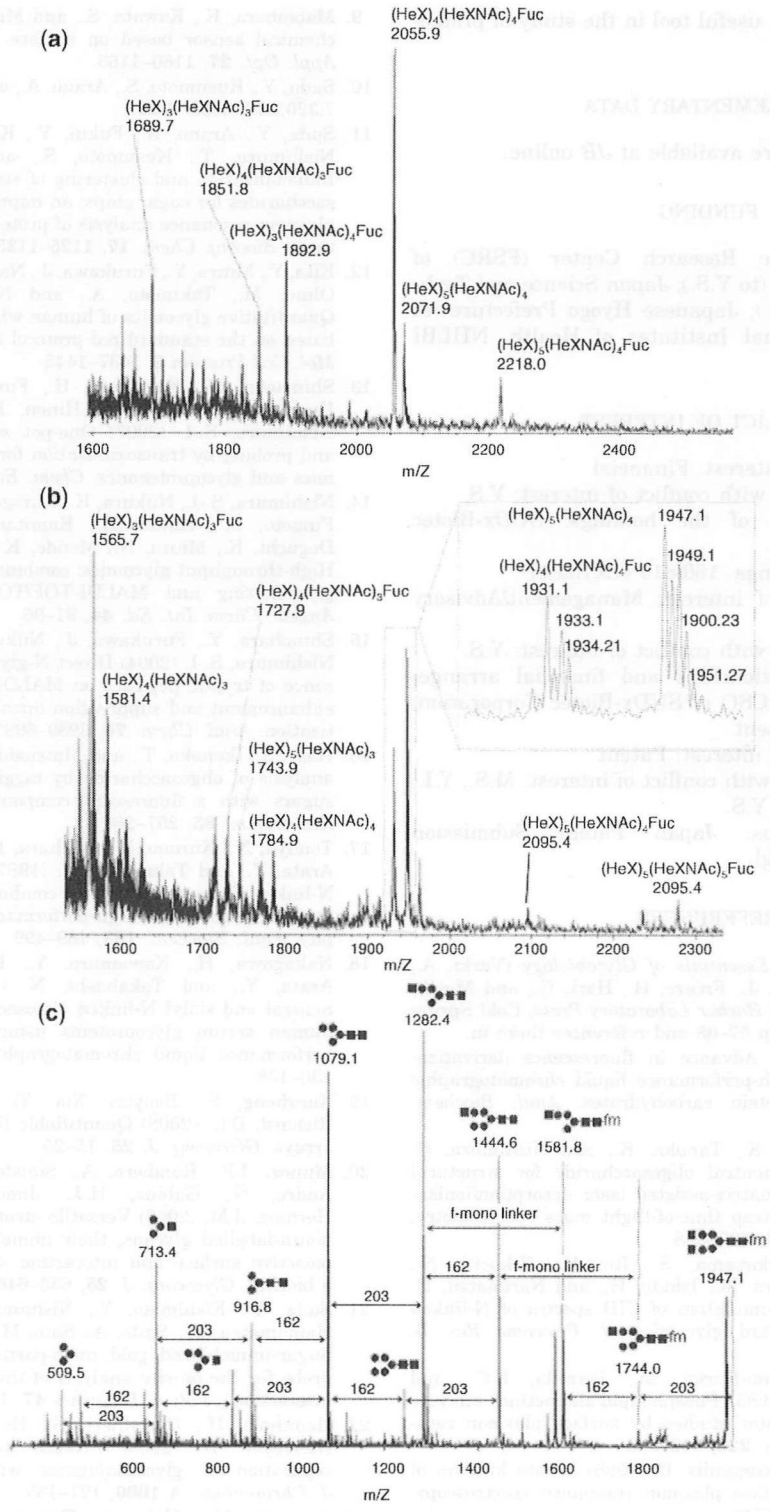

Fig. 4. **MS and MS/MS analyses of labelled N-linked sugar chains from IgG.** From 100 μg of human IgG, N-linked sugar chains were liberated by PNGase F, and concentrated by Blot Glyco (Sumitomo Bakelite Co., Ltd. Tokyo, Japan). The N-glycans were then released in H_2O, lyophilized and transformed to f-mono labelled or aoWRs conjugates as described in MATERIALS AND METHODS section. The labelled N-glycans were examined with mass spectrometry as described above. (a) aoWRs-labelled N-glycans. (b) f-mono labelled N-glycans. (c) MS/MS analysis of a peak ($m/z = 1497.1$) from the MS of f-mono labelled N-linked sugar chain from IgG.

technology should be a useful tool in the study of proteoglycomics.

SUPPLEMENTARY DATA

Supplementary data are available at *JB* online.

FUNDING

The Frontier Science Research Center (FSRC) of Kagoshima University (to Y.S.); Japan Science and Technology Agency (to Y.S.); Japanese Hyogo Prefecture (to Y.S.); and the National Institutes of Health, NHLBI (HL079182 to M.S.).

CONFLICT OF INTEREST

Nature of conflict of interest: Financial

Name of the author with conflict of interest: Y.S.

Entity and nature of the holdings: SUDx-Biotec Corporation

Amount of the holdings: 160/810 (19.753%)

Nature of conflict of interest: Management/Advisory Affiliations

Name of the author with conflict of interest: Y.S.

Nature of the relationships and financial arrangements: President and CSO of SUDx-Biotec Corporation. No financial arrangement.

Nature of conflict of interest: Patent

Name of the author with conflict of interest: M.S., Y.I., N.A., M.B., M.W. and Y.S.

Details and status: Japan Patent Submission #2008-108561 [Pending].

REFERENCES

1. Varki, A. (1999) In *Essentials of Glycobiology* (Varki, A., Cummings, R., Esko, J., Freeze, H., Hart, G., and Marth, J., eds.), *Cold Spring Horbor Laboratory Press*, Cold Spring Harbor, New York, pp 57–68 and references there in.
2. Kalyan, R.A. (2006) Advance in fluorescence derivatization methods for high-performance liquid chromatographic analysis of glycoprotein carbohydrates. *Anal. Biochem.* **350**, 1–23
3. Ojima, N., Masuda, K., Tanaka, K., and Nishimura, O. (2005) Analysis of neutral oligosaccharide for structural characterization by matrix-assisted laser desorption/ionization quadrupole ion trap time-of-flight mass spectrometry. *J. Mass Spectrom.* **40**, 380–388
4. Kameyama, A., Nakayama, S., Ito, H., Kikuchi, N., Angata, T., Nakamura, M., Ishida, H., and Narimatsu, H. (2006) Strategy for simulation of CID spectra of N-linked oligosaccharides toward glycomics. *J. Proteome Res.* **5**, 808–814
5. Plant, A.L., Brigham-Burke, M., Petrella, E.C., and O'Shannessy, D.J. (1995) Phospholipid/alkanethiol bilayers for cell-surface receptor studies by surface plasmon resonance. *Anal. Biochem.* **226**, 342–348
6. Petrlinz, K.A. and Georgiadis, R. (1996) In situ kinetics of self-assembly by surface plasmon resonance spectroscopy. *Langmuir* **12**, 4731–4740
7. Liedberg, B., Nylander, C., and Lundstrom, I. (1983) Surface plasmon resonance for gas detection and biosensing. *Sens. Actuators* **4**, 299–304
8. Flanagan, M.T. and Pantell, R.H. (1984) Surface plasmon resonance and immunosensors. *Electron. Lett.* **20**, 968–970
9. Matsubara, K., Kawata, S., and Minami, S. (1988) Optical chemical sensor based on surface plasmon measurement. *Appl. Opt.* **27**, 1160–1163
10. Suda, Y., Kusumoto, S., Arano, A., and Sobel M., US Patent 7,320,867 (2008. 1.22).
11. Suda, Y., Arano, A., Fukui, Y., Koshida, S., Wakao, M., Nishimura, T., Kusumoto, S., and Michael, S. (2006) Immobilization and clustering of structurally defined oligosaccharides for sugar chips: an improved method for surface plasmon resonance analysis of protein-carbohydrate interactions. *Bioconj. Chem.* **17**, 1125–1135
12. Kita, Y., Miura, Y., Furukawa, J., Nakano, M., Shinohara, Y., Ohno, M., Takimoto, A., and Nishimura, S.-I. (2007) Quantitative glycomics of human whole serum glycoproteins based on the standardized protocol for liberating N-glycans. *Mol. Cell Proteom* **6**, 1437–1445
13. Shimaoka, H., Kuramoto, H., Furukawa, J., Miura, Y., Kurogochi, M., Kita, Y., Hinou, H., Shinohara, Y., and Nishimura, S.-I. (2007) One-pot solid-phase glycoblotting and probing by transoximization for high-throughput glycomics and glycoproteomics. *Chem. Eur. J.* **13**, 4797–4804
14. Nishimura, S.-I., Niikura, K., Kurogochi, M., Matsushita, T., Fumoto, M., Hinou, H., Kamitani, R., Nakagawa, H., Deguchi, K., Miura, N., Monde, K., and Kondo, H. (2005) High-throughput glycomics: combined use of chemoselective glycoblotting and MALDI-TOF/TOF Mass spectrometry. *Angew. Chem. Int. Ed.* **44**, 91–96
15. Shinohara, Y., Furukawa, J., Niikura, K., Miura, N., and Nishimura, S.-I. (2004) Direct N-glycan profiling in the presence of tryptic peptides on MALDI TOF by controlled ion enhancement and suppression upon glycan-selective derivatization. *Anal. Chem.* **76**, 6989–6997
16. Hase, S., Ikenaka, T., and Matsushima, Y. (1978) Structure analysis of oligosaccharide by tagging of the reducing end sugars with a fluorescent compounds. *Biochem. Biophys. Res. Comm.* **85**, 257–263
17. Tomiya, N., Kurono, M., Ishihara, H., Tejima, S., Endo, S., Arata, Y., and Takahashi, N. (1987) Structural analysis of N-linked oligosaccharide by a combination of glycopeptidase, exoglycosidase, and high-performance liquid chromatography. *Anal. Biochem.* **163**, 489–499
18. Nakagawa, H., Kawamura, Y., Kato, K., Shimada, I., Arata, Y., and Takahashi, N. (1995) Identification of neutral and sialyl N-linked oligosaccharide structures from human serum glycoproteins using three kinds of high-performance liquid chromatography. *Anal. Biochem.* **226**, 130–138
19. Xuezheng, S., Baoyun, Xia, Yi, L., David, F.S., and Richard, D.C. (2008) Quantifiable fluorescent glycan microarrays. *Glycoconj. J.* **25**, 15–25
20. Munoz, J.F., Rumbero, A., Sinisterra, V.J., Santos, I.J., Andre, S., Gabius, H.J., Jimenez-Barbero, J., and Hernaiz, J.M. (2008) Versatile strategy for the synthesis of biotin-labelled glycans, their immobilization to establish a bioactive surface and interaction studies with a lectin on a biochip. *Glycoconj. J.* **25**, 633–646
21. Suda, Y., Kishimoto, Y., Nishimura, T., Yamashita, S., Hamamatsu, M., Saito, A., Sato, M., and Wakao, M. (2006) Sugar-immobilized gold nano-particles (SGNP): novel bioprobe for the on-site analysis of the oligosaccharide-protein interactions. *Polym. Preprints* **47**, 156–157
22. Heimholz, H., Cartellieri, S., He, L., Thiesen, P., and Niemeyer, B. (2003) Process development in affinity separation of glycoconjugates with lectins as ligands. *J. Chromatogr. A* **1006**, 127–135
23. Itakura, Y., Nakamura-Tsuruta, S., Kominami, J., Sharon, N., Kasai, K., and Hirabayashi, J. (2007) Systematic comparison of oligosaccharide specificity of Ricinus communis agglutinin I and Eryrina lectins: a search by frontal affinity chromatography. *J. Biochem.* **142**, 459–469